

Key Points:

- Trophic structure of mesozooplankton is regulated by similar environmental factors such as phytoplankton assemblages
- Diazotrophy and nutrient availability correlated with enhanced mesozooplankton carnivory in a complex tropical marine ecosystem
- Mass and energy transfer across trophic levels of planktonic food webs are less efficient in spatially and temporally variable ecosystems

Supporting Information:

Supporting Information may be found in the online version of this article.

Correspondence to:

N. Loick-Wilde,
natalie.loick-wilde@io-warnemuende.de

Citation:

Weber, S. C., Loick-Wilde, N., Montoya, J. P., Bach, M., Doan-Nhu, H., Subramaniam, A., et al. (2021). Environmental regulation of the nitrogen supply, mean trophic position, and trophic enrichment of mesozooplankton in the Mekong River plume and southern South China Sea. *Journal of Geophysical Research: Oceans*, 126, e2020JC017110. <https://doi.org/10.1029/2020JC017110>







Received 20 DEC 2020

Accepted 8 AUG 2021

© 2021. The Authors.

This is an open access article under the terms of the [Creative Commons Attribution License](#), which permits use, distribution and reproduction in any medium, provided the original work is properly cited.

Environmental Regulation of the Nitrogen Supply, Mean Trophic Position, and Trophic Enrichment of Mesozooplankton in the Mekong River Plume and Southern South China Sea

Sarah C. Weber^{1,2} , Natalie Loick-Wilde¹ , Joseph P. Montoya³, Melvin Bach¹, Hai Doan-Nhu⁴ , Ajit Subramaniam⁵ , Iris Liskow¹, Lam Nguyen-Ngoc⁴ , Dirk Wodarg⁶, and Maren Voss¹ 

¹Department of Biological Oceanography, Leibniz Institute for Baltic Sea Research Warnemuende, Rostock, Germany,

²Now at Department of Biology, University of Southern Denmark, Odense, Denmark, ³School of Biological Sciences, Georgia Institute of Technology, Atlanta, GA, USA, ⁴Institute of Oceanography, Vietnam Academy of Science and Technology, Nha Trang, Vietnam, ⁵Lamont-Doherty Earth Observatory, Columbia University, Palisades, NY, USA,

⁶Department of Marine Chemistry, Leibniz Institute for Baltic Sea Research Warnemuende, Rostock, Germany

Abstract The mean trophic position (TP) of mesozooplankton largely determines how much mass and energy is available for higher trophic levels like fish. Unfortunately, the ratio of herbivores to carnivores in mesozooplankton is difficult to identify in field samples. Here, we investigated changes in the mean TP of mesozooplankton in a highly dynamic environment encompassing four distinct habitats in the southern South China Sea: the Mekong River plume, coastal upwelling region, shelf waters, and offshore oceanic waters. We used a set of variables derived from bulk and amino acid nitrogen stable isotopes from particulate organic matter and four mesozooplankton size fractions to identify changes in the nitrogen source and TP of mesozooplankton across these habitats. We found clear indications of a shift in N sources for biological production from nitrate in near-coastal waters with shallow mixed layer depths toward an increase in diazotroph-N inputs in oceanic waters with deep mixed layer depths where diazotrophs shaped the phytoplankton community. The N source shift was accompanied by a lengthening of the food chain (increase in the TP). This may provide further support for the connection between diazotrophy and the indirect routing of N through the marine food web. Our combined bulk and amino acid $\delta^{15}\text{N}$ approach also allowed us to estimate the trophic enrichment (TE) of mesozooplankton across the entire regional ecosystem. When put in the context of literature values, a high TE of 5.1‰ suggested a link between ecosystem heterogeneity and the less efficient transfer of mass and energy across trophic levels.

Plain Language Summary Zooplankton are one of the central pillars of the marine food web and form an important link between the production of organic matter by phytoplankton and biomass at higher trophic levels (e.g., fish). Of particular interest are mesozooplankton (0.2–20 mm in size), which encompass a diverse assemblage of animals utilizing a range of feeding strategies, including herbivory, omnivory, and carnivory. Since mass and energy are lost with each trophic step, their prevailing feeding strategy determines the availability of mass and energy to the upper food web. The exact relationship between carnivores and herbivores in mesozooplankton has so far only been studied with complex experiments or in homogenous environments. We have now resolved zooplankton feeding relationships in a highly dynamic marine environment. Specifically, we used stable nitrogen isotopes in amino acids and bulk organic matter in combination with a habitat-delineating method for phytoplankton to directly determine the ratio of carnivores to herbivores in zooplankton from dynamic habitats in the South China Sea. The mass and energy transfer across trophic levels is less efficient in such variable marine environments compared to stable open ocean systems. These findings represent a big step toward understanding the dynamics of planktonic food webs in general.

1. Introduction

Mesozooplankton occupy a key ecological position in marine systems, and the question of whether carnivory or herbivory prevails in this assemblage can be decisive for the structure and functioning of the entire food web (Steinberg & Landry, 2017). Despite their importance, the mean trophic position (TP) of marine mesozooplankton remains a poorly constrained variable in biogeochemical models (Butenschön et al., 2016; Daewel & Schrum, 2013; Neumann et al., 2002). It is still not well understood how the structure of planktonic food webs responds to changing environmental conditions (Maar et al., 2018; Peck et al., 2018), which has impacts on carbon fluxes, nitrogen (N) cycling, and net primary production (Steinberg & Landry, 2017).

Questions pertaining to mesozooplankton TP persist largely because of the difficulty in determining this measure for natural mesozooplankton populations. ^{15}N natural abundance measurements of bulk mesozooplankton and particulate organic matter (POM) biomass are traditionally used to calculate TP in field mesozooplankton, with POM representing the dietary baseline (Landrum et al., 2011; Montoya et al., 2002). This approach is complicated by the origin, movement, and transformation of nitrogen in the upper water column (Fry & Quiñones, 1994; Goering et al., 1990; Layman et al., 2012), as well as by potential decoupling of bulk $\delta^{15}\text{N}$ signatures given the different N turnover times (life spans) of autotrophs and consumers (Martínez del Río et al., 2009; Montoya, 2007; Tiselius & Fransson, 2015).

Using compound-specific isotope analyses (CSIA) of amino acid nitrogen, it is now possible to directly determine the relative abundance of carnivores and herbivores in zooplankton samples from different field locations. With this information, we can take the next step of relating the effective TPs of zooplankton to the environmental conditions measured in situ (Loick-Wilde et al., 2019), providing much needed insights into the mechanisms driving shifts in TP. The strength of CSIA lies in providing information on both TP and N sources from a single organism/sample, which is achieved with a simple comparison of the $\delta^{15}\text{N}$ values of glutamic acid (Glu) and phenylalanine (Phe) amino acids (McClelland & Montoya, 2002; Mompeán et al., 2016). While Glu is enriched in ^{15}N by $\sim 8.0\%$ per trophic transfer (Chikaraishi et al., 2009), the $\delta^{15}\text{N}$ of Phe remains nearly unchanged when the amino acid (AA) is transferred through the food web and thus reflects the isotopic composition of the primary producers (N-source measure, Chikaraishi et al., 2010). This approach largely eliminates potential sources of error in TP estimates associated with temporal and physiological decoupling between a consumer and its diet, and has been refined and confirmed in numerous field- and lab-based trophic studies over the last decade (reviewed by Glibert et al., 2019 and Ohkouchi et al., 2017).

Though there are still relatively few studies applying these tools to marine zooplankton, considerable progress has been made in resolving the planktonic food web structure in relatively homogenous marine environments like the central gyres of the Atlantic (Mompeán et al., 2016) and Pacific (Hannides et al., 2009, 2013), and in the Baltic Sea (Eglite et al., 2018; Loick-Wilde et al., 2019). Headway has also been made in identifying the environmental factors driving shifts in food web structure. For example, Loick-Wilde et al. (2019) revealed that an increase in the mixed layer depth and higher diazotroph nitrogen inputs from large cyanobacteria were associated with a transition from herbivory to carnivory in mesozooplankton. It was hypothesized that the mesozooplankton did not feed directly on these diazotrophs and instead grazed on the associated heterotrophic microbial community supported by diazotroph N. In turn, the shift to grazing on heterotrophs increased the apparent TP of mesozooplankton. Whether parts of this mechanism, found in a comparatively stable environment, also apply to other more variable marine ecosystems is currently unknown. The central goals of this study are to (a) determine whether it is possible to identify changes in planktonic food web structure (i.e., the ratio of herbivores to carnivores) using CSIA in more physicochemically variable systems, and if so, (b) identify the environmental factors driving these shifts.

The southwestern region of the South China Sea (SCS), off the coast of south-central Viet Nam, represents an ideal site for exploring these questions. This highly productive and dynamic region receives inputs of new nitrogen through wind-induced and dynamical upwelling and through biological N_2 fixation promoted by discharges of the Mekong River during the southwest monsoon (SWM) season (Bombar et al., 2010; Dipner et al., 2007; Grosse et al., 2010; Voss et al., 2006). In June 2016, this region was characterized by a suite of phytoplankton assemblages including nitrate-utilizing and N_2 -fixing communities that were associated with distinct habitat types (Weber et al., 2019). These habitat types, which partitioned the sampled stations

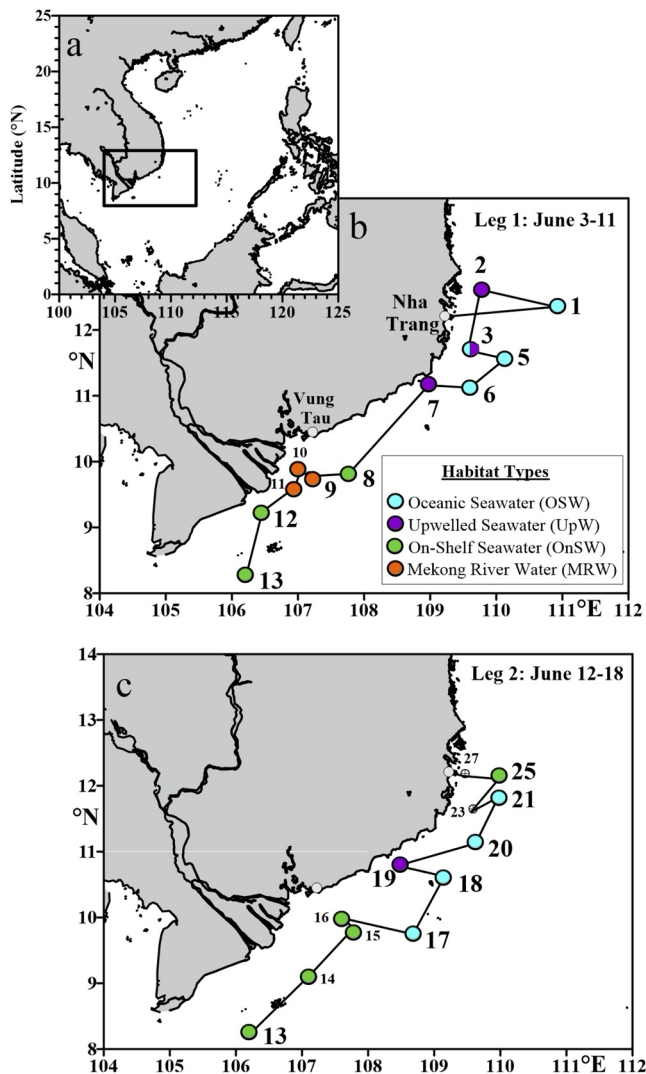


Figure 1. Overview (a) and station maps from leg 1 (b) and leg 2 (c) including the cruise track off south-central Viet Nam. Note that Stations 8 and 15 as well as Stations 6 and 20 are coincident in space but were sampled days apart. Colors indicate habitat types after Weber et al. (2019) (see legend). Stations 23 and 27 could not be assigned habitat types due to inadequate sampling at these sites. Waters at Station 3 transitioned from the Oceanic Seawater habitat to the Upwelled Seawater habitat over the duration of sampling. Stations for amino acid-specific nitrogen stable isotope analyses (CSIA): enlarged. Stations without CSIA: small.

into statistically robust groups, corresponded to the primary end members sampled in the area: Mekong River water (MRW), upwelled water (UpW), and oceanic seawater (OSW), along with a mixed-source habitat termed on-shelf waters (OnSW). When combined with phytoplankton community data, the habitats enabled a clearer understanding of how phytoplankton distributions and community composition varied across the hydrographically complex environment.

Here, we assess the impact of N_2 fixation and the trophic structure of the planktonic food webs in these different habitats using bulk $\delta^{15}N$ values and two AA nitrogen stable isotope-based biogeochemical measures ($\delta^{15}N$ -Phe and $TP_{Glu/Phe}$) from stations across the southwestern SCS. We relate our isotope-based measures to the habitat types of Weber et al. (2019) and to additional environmental data, allowing us to evaluate how the trophic structure of mesozooplankton can change along with the mixed layer depth, diazotroph biomass, nutrient availability, and phytoplankton community structure in a highly dynamic aquatic ecosystem like the Mekong River plume and adjacent SCS.

2. Materials and Methods

2.1. Characterization of Study Area and Sampling Stations

Samples of seawater and plankton were collected on R/V Falkor cruise FK160603 (3–18 June, 2016) to the SCS off southern central Viet Nam (Figure 1). Stations were characterized according to statistically determined habitat types developed by Weber et al. (2019). This approach extends traditional water mass characterizations (Dippner & Loick-Wilde, 2011; Dippner et al., 2007) by adding integrative and emergent properties including mixed layer depth (MLD), nitrate availability, and depth of the Chl. *a* maximum (ChlMD) to sea surface salinity (SSS) and temperature (SST) water mass information. To estimate nitrate availability in the upper water column, Weber et al. (2019) developed a nitrate availability index (NAI) defined as,

$$NAI = \begin{cases} [NO_{2/3}], & \text{if } [NO_{2/3}]_{\text{surface}} \geq 0.5 \mu M \\ -Z_{[NO_{2/3}]} = 2 \mu M, & \text{if } [NO_{2/3}]_{\text{surface}} < 0.5 \mu M \\ -Z_{\text{bottom}}, & \text{else} \end{cases} \quad (1)$$

where $[NO_{2/3}]$ is the sum of the concentrations of nitrate and nitrite and Z is the water column depth, positive downward. The index scales directly with nitrate availability in surface waters, where positive NAI values reflect significant surface $[NO_{2/3}]$, indicating a relief from nitrate limitation. In contrast, negative NAI values reflect a lack of nitrate at the surface, and NAI becomes increasingly negative as the nitracline depth increases. For more on NAI, please refer to Weber et al. (2019).

Due to the dynamic nature of the region, we report the habitat type for each individual hydrocast. All CTD casts and mesozooplankton tows are labeled and discussed according to their unique “station.event” number, where the event refers to an individual sampling activity at a given station. Stations 23 and 27 could not be assigned habitat types due to inadequate sampling at these sites.

2.2. Station Seawater and Plankton Sampling

Water samples were obtained using a Seabird CTD-rosette system outfitted with a sensor for chlorophyll *a* fluorescence (in the following Chl. *a*). Mixed layer depths (MLD) were estimated from the maximum in

the buoyancy frequency of the water column. Nutrient (SiO_2 , $\text{NO}_3 + \text{NO}_2$ and PO_4) samples were filtered (0.2 μm cellulose acetate) and frozen at sea, and then analyzed ashore after Grasshoff et al. (1983). Here, we report on nutrient concentrations from samples taken in the upper 100 m. Nitrogen isotope analyses of nitrate were carried out using the denitrifier method (Casciotti et al., 2002; Sigman et al., 2001, see also Supporting Information S1), with a focus on measurements on water collected from the upper 150 m of the water column (10 stations) where the upwelling water mass is positioned (Dippner & Loick-Wilde, 2011; Dippner et al., 2007).

Samples for phytoplankton enumeration were collected from surface CTD bottles, and further details on how phytoplankton were enumerated and converted to cell carbon can be found in the supporting information. Here, we report the relative biomass of diazotrophs (wt%) as the ratio of diazotroph biomass to whole community biomass on the basis of cell carbon. 'Diazotrophs' refer to the most abundant species that were enumerable with microscopy (cells > ca. 5 μm), which excludes unicellular groups. The most abundant species were *Trichodesmium* spp. and the diatom-diazotroph association (DDA) host species *Rhizosolenia clevei* var. *communis*, and *Hemiaulus membranaceus*. These DDA host species were typically found with one or more diazotrophic symbionts and their populations commonly had infection rates of 80%–100% (Hai Doan-Nhu, Sarah Weber, unpublished data).

Samples of particulate organic matter (POM) for elemental and bulk isotope analyses were collected from the same depths as the nutrient samples. Seawater (1–19 L) was filtered through precombusted (450°C for 2 h) 47-mm GF/F filters (0.7 μm nominal pore size) using gentle pressure filtration (5–10 psi). Filter samples were dried at 60°C onboard and stored over desiccant for analysis ashore. At selected stations, additional samples of POM for CSIA were collected by gentle pressure filtration of 20–60 L of seawater from either the surface or the chlorophyll-maximum through a series of preweighted 47-mm polycarbonate filters (Whatman Nuclepore, 0.2 μm). Samples were frozen at -20°C and dried at 60°C ashore.

Zooplankton for elemental, bulk isotope, and compound specific isotope analyses were collected in vertical tows around local noon and local midnight with a 0.5 m^2 ring net (200 μm mesh size) equipped with a USBL transponder and at a towing speed of 1.0 m s^{-1} . According to Kiørboe et al. (2014) and Clark et al. (2001), we may have undersampled animals within the 1,000–2,000 μm and >2,000 μm size fractions due to net avoidance. We sampled through the upper 100 m of the water column or to ~ 10 m above bottom at shallower stations. Animals were size-fractionated using a graded series of Nitex sieves with mesh sizes of 2,000, 1,000, 500, and 250 μm and dried onboard at 60°C for 48 h. Dry samples were ground to a fine powder, then stored in precombusted aluminum foil (450°C for 2 h) at -20°C for the duration of the cruise.

2.3. Elemental and Biochemical Analyses of Plankton Samples

All elemental concentration and bulk stable isotope measurements of POM and size-fractionated zooplankton samples were made by elemental analysis with coupled isotope ratio mass spectrometry (EA-IRMS). Analyses were carried out using a Thermo Scientific Delta V Advantage interfaced to a Flash 2000 elemental analyzer in Warnemünde, Germany or a Micromass Isoprime IRMS coupled to a Carlo Erba NA2500 elemental analyzer in Atlanta, GA, USA. The overall precision of our bulk isotopic analysis is better than $\pm 0.2\text{‰}$ for $\delta^{13}\text{C}$ and $\delta^{15}\text{N}$ for both the instruments, which were cross-calibrated by running splits of the same standard sets.

The $\delta^{15}\text{N}$ values of trifluoroacetyl/isopropyl ester (TFA) AA derivatives (Hofmann et al., 2003; Veuger et al., 2005) were measured on a Thermo GC Isolink CN with Trace 1310 (GC), coupled through a ConFlo IV combustion interface (C) to a Mat 253 (IRMS, all Thermo Fisher Scientific GmbH, Dreieich, Germany) in Warnemünde. The precision of our GC-C-IRMS measurements varied among individual AAs and sample type but the standard deviation of 2–5 analyses typically was $\leq 1.0\text{‰}$. Due to the resource intensive nature of this approach, CSIA analyses were performed on only a subset of POM and zooplankton samples, which included POM from the surface and Chl. *a* maximum and mesozooplankton from the 1,000–2,000 μm size fraction. This size fraction was chosen because it provided good coverage across the various habitats (zooplankton in the larger size fractions were not always present at adequate abundances) and because samples from this size fraction had minimal phytoplankton contamination (explained in more detail below). In total, nine POM samples from six stations (Table S1) and 21 zooplankton samples from 15 stations (Ta-

ble S2, Figure 1) were analyzed for CSIA. Individual nitrogen stable isotopes of 12 AAs included the so-called “source” AAs glycine (Gly), lysine (Lys), phenylalanine (Phe), and tyrosine (Tyr); the “trophic” AAs alanine (Ala), aspartic acid (Asp), glutamic acid (Glu), isoleucine (Ile), leucine (Leu), proline (Pro), and valine (Val); and the “metabolic” AA threonine (Thr), categorized by Germain et al. (2013), McClelland and Montoya (2002), and Chikaraishi et al. (2009) according to the sensitivity of each AA to trophic enrichment in ^{15}N . Asp and Glu also include the amide forms asparagine and glutamine, respectively, with the N isotopic signature coming only from the α -amino-N from both the compounds as the amide N is lost during hydrolysis. Details of the EA-IRMS and GC-C-IRMS analyses are provided in the supporting information.

2.4. Biogeochemical Measures

For comparison with the zooplankton data, we calculated the concentration- and depth-weighted mean $\delta^{15}\text{N}$ value of POM by vertically integrating discrete samples collected from the upper 100 m of the water column (or less at shallower stations) for each station (in the following POM) (Equation S3). The relative contribution of diazotroph N ($\%N_{\text{diaz}}$) to the bulk $\delta^{15}\text{N}$ values of POM and zooplankton was calculated using the N isotope mass balance approach of Landrum et al. (2011) including ecosystem-specific POM and zooplankton $\delta^{15}\text{N}$ end member values (Equation S4).

The $\delta^{15}\text{N}$ -Phe values of the subset of discrete POM and zooplankton samples for CSIA analyses were used as time-integrating proxies for the dominant inorganic nitrogen source sustaining planktonic food webs across the investigation area (Loick-Wilde et al., 2019; McClelland & Montoya, 2002; McMahan et al., 2015). The average TP of the subset of POM and zooplankton samples for CSIA analyses were estimated based on the isotopic contrast between Glu and Phe (Equation S5). This is generally accepted as the best pair of AAs for plankton TP estimates for identifying autotrophy (TP of 1.0), herbivory (TP of 2.0), and first level carnivory (TP of 3.0) (e.g., Chikaraishi et al., 2009; Mompeán et al., 2016), as well as their mixtures like mixotrophy ($1.0 < \text{TP} < 2.0$) or omnivory ($2.0 < \text{TP} < 3.0$) (e.g., Eglite et al., 2018; Ferrier-Pagès et al., 2021; Fujii et al., 2020; Hannides et al., 2009). Alternative TP calculations were tested, including TPs based on $\delta^{15}\text{N}$ -Ala and $\delta^{15}\text{N}$ -Phe ($\text{TP}_{\text{Ala/Phe}}$), which would help to identify a significant impact of protozoans on the food web (Décima et al., 2017), yet no indication for this process was found (Figure S4a). Details of the TP calculations and evaluation of heterotrophic protist activity can be found in the supporting information. Standard error (SE) in TP estimations computed by propagation of analytical error in the individual AA determinations, did not exceed 0.1 TP with the exception of one POM sample (Stn. 5) and one mesozooplankton sample (Stn. 1), where SE was 0.2 TP in both the cases.

Detritivory may also be a common feeding mode, though one which cannot be resolved by TP estimation alone (Steffan et al., 2017). Rather, the degree of microbial reprocessing of food in the animal's diet can be estimated by the microbial resynthesis proxy ΣV (Eglite et al., 2019; McCarthy et al., 2007). ΣV quantifies the extent of heterotrophic alteration of detrital material before it is consumed by an animal (detritivory) and thus provides an integrated measure of the full range of trophic behavior of an animal. ΣV is only considered to be a robust proxy for detritivory if unrelated to TP since trophic effects influence both estimations (Ohkouchi et al., 2017). Details of the ΣV calculations and evaluation of detritivory can be found in the supporting information (Equation S6 and Figure S4b).

2.5. Identification of Outliers

We used a two-step process based on sample C:N ratios (Steinberg & Saba, 2008) and on bulk $\delta^{15}\text{N}$ values in relation to the MLD (Loick-Wilde et al., 2019; Voss et al., 2006) to identify bulk POM and zooplankton samples that should be excluded from further analysis due to contamination with fish (C:N < 4.0) or large phytoplankton (C:N > 5.4) or influence from transient events of isotopic fractionation related to nitrate uptake. We found that across all plankton compartments, $\delta^{15}\text{N}$ data from Stn. 6 deviated from the generally tight relationship between $\delta^{15}\text{N}$ and MLD (Figure 2). Removal of $\delta^{15}\text{N}$ data from Stn. 6 could be justified based on the environmental conditions and type of plankton community sampled, as addressed in detail below. Details of the outlier identification can be found in the supporting information and Figure S1.

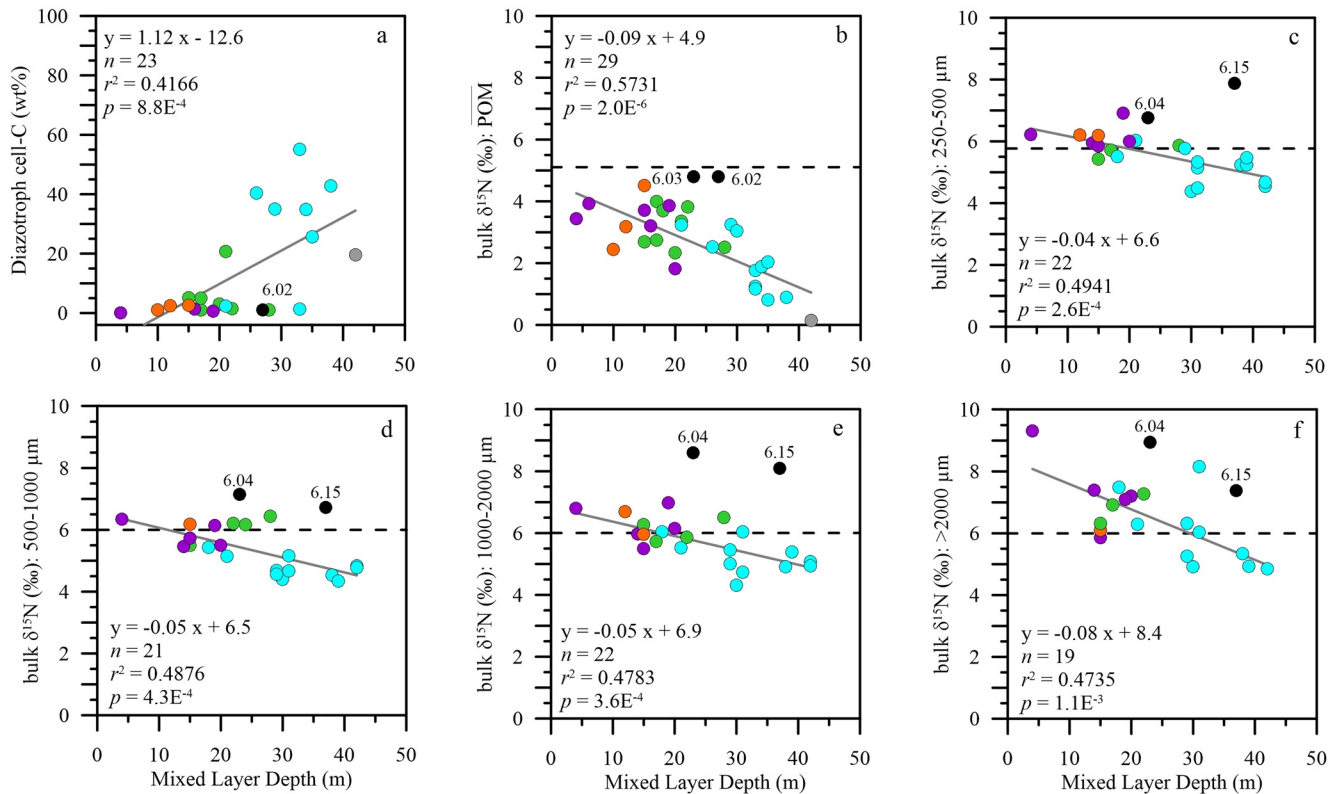


Figure 2. Relationship of surface diazotroph biomass (wt%) (a) and $\delta^{15}\text{N}$ values of POM samples (b) and four mesozooplankton size fractions with mixed layer depth: (c) 250–500 μm ; (d) 500–1,000 μm ; (e) 1,000–2,000 μm , and (f) >2,000 μm size fractions. Regression lines (continuous lines) and details are shown. Dashed lines represent the ecosystem-specific reference values used for determining % diazotroph N in samples: 5.1‰ for POM is the $\delta^{15}\text{N}$ of upwelling nitrate, and 5.8‰ and 6.0‰ are the respective $\delta^{15}\text{N}$ values of <500 μm and >500 μm size fractions of mesozooplankton dependent on nitrate-based production (see Supporting Information S1). Circle colors indicate habitat types as in Figure 1. Black circles indicate the high $\delta^{15}\text{N}$ values from Stn. 6 that were excluded from linear regressions.

2.6. Statistical Analysis

To test for differences in bulk $\delta^{15}\text{N}$ values between size fractions, we used a one-way analysis of variance (ANOVA, $\alpha = 0.05$). Normality of data was confirmed with the Anderson-Darling tests. Since variance was not homogenous across size fractions, a Welch correction was applied to the ANOVA, which was followed by a Games-Howell post-hoc analysis. For these analyses, we only included tows for which bulk $\delta^{15}\text{N}$ data from all four mesozooplankton size fractions were available ($n = 16$).

Multivariate linear correlations on normalized data (scaled to zero mean and unit variance) were used to identify the biotic and abiotic factors that affect the mean N-source and TP of the 1,000–2,000 μm size fraction of zooplankton across the four different habitat types. The analysis comprised a total of 13 variables measured across 15 stations (excluding Stn. 6) from all the four habitat types (Table 1). Since the mesozooplankton isotopic measures are integrated over the depth interval sampled by our net tows, the environmental variables were also depth-integrated where appropriate in order to relate them more directly to the zooplankton measures (Table 1). Given the strong relationship between bulk $\delta^{15}\text{N}$ values of plankton and the MLD, and the role of the MLD in regulating nutrient supply to the phytoplankton community (Gattuso et al., 2015; Hutchins & Fu, 2017; Jewett & Romanou, 2017; Paerl & Huisman, 2008; Roy et al., 2011) and vertical migration of zooplankton (Eglite et al., 2018; Schnetzer & Steinberg, 2002) in the upper water column, we integrated the environmental variables over the mixed layer for the regression analyses. We tested other integration depths including the net tow bottom depth and ChIMD, but these integrations did not produce significant relationships with mesozooplankton N-source and TP measures (not shown). Therefore, we only report the regression analyses with the MLD-integrated environmental values. All statistical analyses were carried out using JMP Pro 14 (SAS Institute Inc., USA).

Table 1

Station Environmental Characteristics in the Surface Mixed Layer and Isotopic Measures of the Mesozooplankton 1,000–2,000 μm Size Fraction From the Upper 100 m (or to the Bottom if Shallower)

Habitat	Station	MLD	$\overline{\text{Temp}}$	$\overline{\text{Sal}}$	NAI	$\overline{\text{PO}_4^{3-}}$	$\overline{\text{SiO}_2}$	$\overline{\text{DIN}}$	ChlMD	$\overline{\text{FL}}$	$\delta^{15}\text{N}$			
											bulk _{zp}	Phe _{zp}	Glu _{zp}	TP _{zp}
MRW	9	15	30.8	32.5	0.5	0.17	9.68	0.16	6	0.18	6.0	5.8	14.8	1.7
OnSW	12	22	30.3	33.3	−22.0	0.11	5.23	0.00	21	0.04	5.9	4.5	16.4	2.1
OnSW	13	28	29.9	33.4	−27.9	0.14	5.35	0.38	15	0.03	6.5	6.7	16.2	1.8
OnSW	25	15	30.8	33.4	−40.0	0.08	2.94	0.00	34	0.01	6.3	4.5	17.6	2.3
UpW	2	14	29.0	33.9	−44.9	0.07	2.70	0.27	46	0.00	6.0	3.9	14.2	1.9
UpW	2	14	29.0	33.9	−44.9	0.07	2.70	0.27	46	0.00	5.5	1.7	14.7	2.3
UpW	3.12	20	25.8	34.1	0.8	0.08	2.80	0.50	51	0.01	6.2	3.3	14.4	2.0
UpW	7	4	25.3	34.2	−29.2	0.10	4.08	0.03	13	0.02	6.8	5.4	15.9	1.9
UpW	19	19	25.6	34.1	−27.8	0.13	4.38	0.33	22	0.06	7.0	5.8	16.9	2.0
OSW	1	33	30.1	33.9	−64.7	0.06	2.55	0.04	58	0.00	5.1	2.7	14.3	2.1
OSW	1	33	30.1	33.9	−64.7	0.06	2.55	0.04	58	0.00	4.9	2.3	15.3	2.3
OSW	3.01	30	26.7	34.0	−54.8	0.05	2.53	0.04	55	0.01	6.0	1.5	14.0	2.2
OSW	5.04	21	29.4	33.7	−67.3	0.08	4.40	0.21	75	0.01	6.0	1.2	14.6	2.3
OSW	5.16	21	29.4	33.7	−67.3	0.08	4.40	0.21	75	0.01	5.5	1.7	15.7	2.4
OSW	6	23	28.3	33.7	−61.5	0.08	2.59	0.15	31	0.03	8.1	2.0	13.7	2.1
OSW	6	23	28.3	33.7	−61.5	0.08	2.59	0.15	31	0.03	8.6	2.4	15.3	2.2
OSW	17	30	30.2	33.6	−50.8	0.07	3.61	0.20	64	0.01	4.3	2.3	16.1	2.4
OSW	17	26	30.1	33.6	−85.3	0.09	4.37	0.19	56	0.01	4.7	3.3	13.5	1.9
OSW	18.04	38	29.1	33.8	−50.5	0.08	3.48	0.19	47	0.03	4.9	6.1	20.8	2.5
OSW	20	35	30.1	33.6	−60.0	0.08	3.79	0.19	68	0.01	5.4	2.2	15.6	2.3
OSW	21	33	28.1	34.0	−49.5	0.11	3.73	0.31	45	0.03	5.0	5.8	15.0	1.8

Note. Fluorescence is in relative units. Overlined variables were integrated through the mixed layer. All variables were included in the multivariate analysis, whereas stations with outliers were excluded (italicized).

ChlMD, chlorophyll max. depth; DIN, dissolved inorganic nitrogen; FL, fluorescence; Glu, glutamic acid; MLD, mixed layer depth; MRW, Mekong River water; NAI, nitrate availability index; OnSW, on-shelf seawater; OSW, oceanic seawater; Phe, phenylalanine; PO_4^{3-} , phosphate; Sal, salinity; SiO_2 , silicate; Temp, temperature; TP, trophic position; UpW, upwelled water; and zp, zooplankton.

3. Results

We characterized the stations according to the four habitat types delineated by Weber et al. (2019): MRW, OnSW, UpW, and OSW (Figure 1). This approach clearly identified stations influenced by the Mekong River (MRW) in close proximity to the river mouth (Figure 1b). The majority of OnSW stations were situated along the southern shelf, whereas to the north, waters along the coast were influenced by upwelling (UpW) and those farther offshore were indicative of oceanic conditions (OSW). Though we could not clearly identify the Mekong River plume with remote sensing techniques, SST documented the fluctuations in the surface upwelling signal, where cooler temperatures are indicative of upwelled waters (Figure S2). Water samples from the upwelling water mass (~60–150 m) showed $\delta^{15}\text{N}$ values for nitrate of $5.1 \pm 0.4\text{‰}$, whereas nitrate from shallower depths was enriched in ^{15}N : Stns. 2 (9.5‰), 3 (8.3‰), and 7 (8.0‰) (Figure S3).

3.1. Trends in Diazotroph Biomass and Bulk $\delta^{15}\text{N}$ Values of POM and Zooplankton

We extended the habitat type approach to biogeochemical processes in higher trophic levels by identifying habitat-specific nitrogen sources for particles and mesozooplankton. Trends in these measures become even more apparent when plotted against MLD, which is known to govern N availability and is a defining

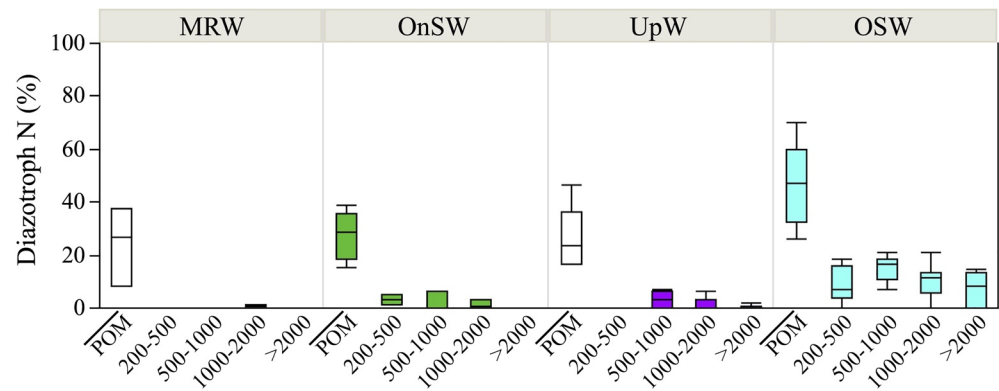


Figure 3. Diazotroph N (%) contribution to particulate organic matter (POM) integrated over the zooplankton tow depth (POM) and four mesozooplankton size fractions, where samples are grouped by habitat type. Samples from Stn. 6 with anomalously high $\delta^{15}\text{N}$ values (see Figure 2) were excluded. Boxes without color (MRW and UpW POM) likely have falsely high diazotroph N contributions due to nitrate fractionation (see Discussion subsection “Nitrogen supply in different habitat types” for details).

variable in habitat delineations. We found significant linear relationships of MLD with the relative biomass of diazotrophs and with the depth-integrated bulk $\delta^{15}\text{N}$ values of all the five planktonic compartments (Figure 2). Specifically, diazotroph relative biomass increased directly with MLD and reached up to 20%–60% within the OSW habitat. In contrast, bulk $\delta^{15}\text{N}$ values of POM and the four mesozooplankton size fractions varied indirectly with MLD and tended to be lowest at OSW stations. The anomalous Stn. 6 had consistently high bulk $\delta^{15}\text{N}$ values in all five plankton compartments, which is in stark contrast to the otherwise low bulk $\delta^{15}\text{N}$ values at the other OSW habitat stations (Figure 2). Excluding these outliers, bulk $\delta^{15}\text{N}$ values of mesozooplankton varied between 4.3 and 9.3‰ (Figure 2). An analysis of variance revealed statistically significant differences in bulk $\delta^{15}\text{N}$ values between the four mesozooplankton size fractions, Welch’s $F(3, 102,71) = 13,00, p < 0.001$. A post-hoc analysis showed that only the $>2,000\ \mu\text{m}$ and $500\text{--}1,000\ \mu\text{m}$ size fractions differed ($p < 0.01$).

Applying a simple isotope mixing model that utilizes ecosystem-specific reference values (Equation S4), we identified clear habitat-specific differences in the contribution of diazotroph N to the plankton compartments (Figure 3). POM included up to 70% of N from N_2 fixation at OSW habitat type stations. In contrast, mesozooplankton received at most 20% of their nitrogen from N_2 fixation in OSW waters. But, while the mixing model also generated diazotroph N inputs into particles for MRW, OnSW, and UpW stations, diazotroph N was hardly incorporated into mesozooplankton outside the OSW waters. Finally, the anomalous Stn. 6 was the only OSW type station without clear diazotroph N inputs into either particles or mesozooplankton (not shown).

3.2. Nitrogen Sources and Food Web Structure of Mesozooplankton

A subset of the POM and zooplankton were additionally analyzed with CSIA, which included samples from most habitat types (except from UpW waters for POM, Figure 4). From these analyses, the N source measure $\delta^{15}\text{N}\text{-Phe}$ and the food web structure measure TP were determined for both the pools. The $\delta^{15}\text{N}\text{-Phe}$ values of POM and zooplankton samples confirmed the pattern in the bulk $\delta^{15}\text{N}$ measurements and revealed large differences both among stations and between compartments (Figure 4, Tables S1 and S2). The $\delta^{15}\text{N}\text{-Phe}$ values in POM from both surface and deep Chl. *a* maxima were clearly lower than the values in zooplankton and ranged from -2.0‰ to 1.6‰ with a mean value of $0.4 \pm 1.0\text{‰}$. The $\delta^{15}\text{N}\text{-Phe}$ values in the zooplankton $1,000\text{--}2,000\ \mu\text{m}$ size fraction covered a much wider range from 1.2‰ to 6.7‰ with a mean value of $3.6 \pm 1.8\text{‰}$. For POM, no clear habitat-specific expression of $\delta^{15}\text{N}\text{-Phe}$ values was found, although the minimum value was measured in surface waters at an OSW station (Stn. 17). In contrast, the mesozooplankton $\delta^{15}\text{N}\text{-Phe}$ values showed a stronger relationship with habitat types, with values clearly below 5‰ mainly at OSW stations and values close to or $>5\text{‰}$ mainly at MRW, OnSW, and UpW stations.

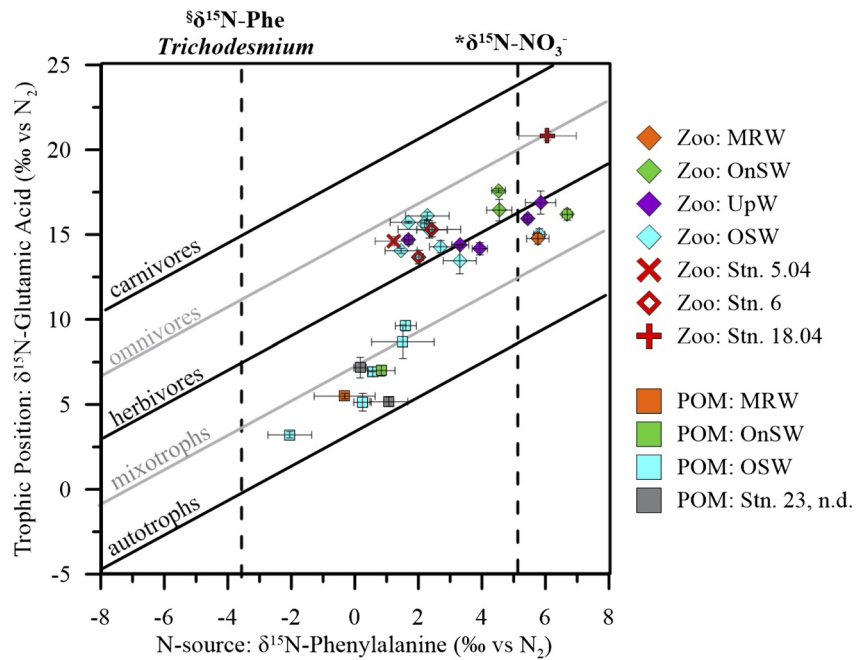


Figure 4. Cross-plot for the $\delta^{15}\text{N}$ values of glutamic acid (Glu) and phenylalanine (Phe) for particulate organic matter (POM) and the mesozooplankton 1,000–2,000 μm size fraction from four different habitats. Trophic isoclines with a slope of 1.0 and a y-intercept interval of 7.6‰ represent different trophic positions (TPs = 1.0, 1.5, 2.0, 2.5, and 3.0) according to Chikaraishi et al. (2009); Eglite et al. (2018); Ferrier-Pagès et al. (2021); Fujii et al. (2020); Hannides et al. (2009); and Mompeán et al. (2016). Vertical black dashed lines: $\delta^{15}\text{N}$ Phe values in N_2 -fixing *Trichodesmium* (McClelland et al., 2003) and $\delta^{15}\text{N}$ value for deep water nitrate from this cruise. Zooplankton samples from outlier Stns. 5.04, 6, and 18.04 are shown individually.

The estimated TPs of POM samples using the $\text{TP}_{\text{Glu/Phe}}$ approach ranged from 1.1 to 1.6 (Figure 4, Table S1), thus mostly reflecting material of autotrophic and mixotrophic origin (Ferrier-Pagès et al., 2021; Fujii et al., 2020; Steffan et al., 2017). The TP of zooplankton in the 1,000–2,000 μm size fraction ranged from 1.7 to 2.5 (Figure 4, Table 1) reflecting mainly herbivorous and some omnivorous (OSW Stns. 5.16, 17, and 18.04) feeding behaviors. Interestingly, no clear signal of predominantly carnivorous feeding behavior ($\text{TP} \geq 3.0$) was found in any of the zooplankton samples. The standard errors in the estimation of TP were quite small for POM and mesozooplankton, usually not exceeding 0.1 TP indicating quite high precision in the ability of CSIA to resolve TP values despite the fairly narrow range in overall TP values.

The highly significant relationship between ΣV and TP values for the majority of mesozooplankton samples implied that detritivory was not a significant source of variation in our data set (Figure S4b, Ohkouchi et al., 2017). Samples from Stns. 5.04 and 18.04, however, were clear exceptions, where their anomalously high ΣV values (2.3 and 2.5, respectively) relative to TP (2.3 and 2.5, respectively) strongly indicated the incorporation of a microbially altered diet (Figure S4 and Table S2).

3.3. Environmental Controls on Food Web Structure

Multivariate linear correlations were used to identify the environmental controls on mesozooplankton food web structure according to the amino acid N-source measure ($\delta^{15}\text{N}\text{-Phe}_{\text{zp}}$) and TP estimates (TP_{zp}) (Figure 5, Table 1). Of the environmental variables assessed in the correlation analysis, those related to nutrient availability tended to correlate the strongest with zooplankton isotope measures. $\overline{\text{PO}_4^{3-}}$ correlated inversely with TP_{zp} ($r^2 = 0.41$), whereas both $\overline{\text{PO}_4^{3-}}$ and NAI varied directly with $\delta^{15}\text{N}\text{-Phe}_{\text{zp}}$ ($r^2 = 0.67$ and 0.32, respectively). ChIMD, which indirectly reflects nutrient availability through phytoplankton distributions, also correlated with $\delta^{15}\text{N}\text{-Phe}_{\text{zp}}$ ($r^2 = 0.72$) and TP_{zp} ($r^2 = 0.41$), where $\delta^{15}\text{N}\text{-Phe}_{\text{zp}}$ values decreased and TP_{zp} increased with deepening ChIMDs. Interestingly, $\delta^{15}\text{N}\text{-Phe}_{\text{zp}}$ showed no significant relationship with MLD and correlated weakly with $\delta^{15}\text{N}\text{-bulk}_{\text{zp}}$ ($r^2 = 0.30$) but varied rather strongly and indirectly with TP_{zp} ($r^2 = 0.61$).

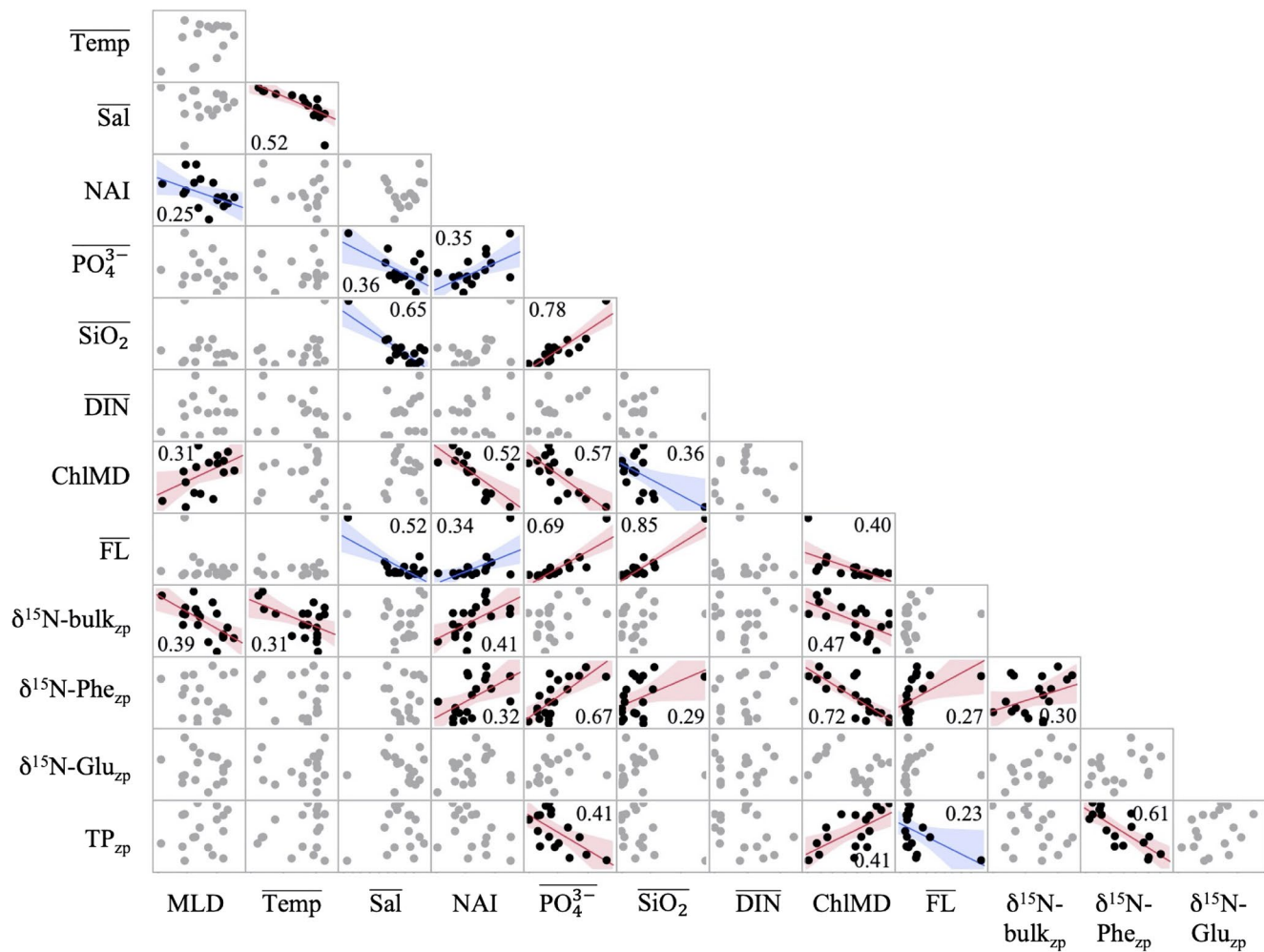


Figure 5. Multivariate analysis of environmental factors regulating the planktonic food web structure and its nitrogen supply. Variables correspond to Table 1. Regression lines, 95% confidence intervals (shaded regions), and r^2 values are shown for statistically significant ($p < 0.05$) relationships. Since we have zooplankton amino acid isotope data from only one MRW station (Stn. 9), regressions were tested both with and without this station. Regressions in blue were significant only when the MRW station was included, whereas those in red were significant regardless of its inclusion. Stns. 5.04 and 18.04 were excluded from $\delta^{15}\text{N-Glu}_{\text{zp}}$ and TP_{zp} analyses due to their high zooplankton ΣV values (see main text).

4. Discussion

Stratification and diazotrophy have been identified as key environmental and biological controls on the primary N source to the pelagic food web in relatively stable environments. These factors consequently shape mass and energy flow at the base of the food web, causing a trophic shift in the mesozooplankton. Here, we have investigated how these and other factors characterize trophodynamics in spatially and temporally variable systems, using the physicochemically diverse waters of the southwestern SCS as a test system.

4.1. Dynamic Nature of the Ecosystem

The distribution of different water masses and therefore, nutrient sources to the SCS during this cruise reflected both the season and recent weather conditions. In June, during the early SWM season, the Mekong River began its transition into the high flow period (Thi Ha et al., 2018) and the wind-induced coastal upwelling system was established. Though both the Mekong River plume and upwelling were hydrographically detectable during the cruise, both features were likely suppressed due to an ENSO event during the previous year (Chao et al., 1996; Dippner et al., 2013; Dippner et al., 2007), which is known to lower precipitation and weaken monsoon winds. As a consequence of the timing of the cruise at the very start of the SWM and

during a post-ENSO year, the Mekong River plume and its impact on the local waters were restricted to the river mouth and nearby coastline (Figure 1).

The general distribution of surface water masses was in accordance with previous post-ENSO SWM seasons (Dippner & Loick-Wilde, 2011), but the highly dynamic nature of the system was exemplified by repeated satellite SST images (Figure S2). The images show considerable small-scale fluctuations in the position of the upwelling front, along with the development of a typical offshore jet at $\sim 12.5^{\circ}\text{N}$ (Dippner et al., 2007; Wu et al., 1998) over the course of the cruise (Figure S2d). Physicochemical variability on these timescales has important implications for phytoplankton growth, but the impact of this variability on planktonic food web structure and dynamics can be difficult to resolve. Weber et al. (2019) have previously shown that a habitat type approach using a combination of variables that integrate over varying timescales generates a biologically relevant framework for evaluating phytoplankton communities and the environmental processes shaping them. Using this framework in combination with tools like remote sensing allows us to untangle the distributions of major phytoplankton groups in the SCS and provides a robust context for interpreting bulk and amino acid specific nitrogen stable isotope signatures in the five plankton compartments included in this study.

4.2. Nitrogen Supply in Different Habitat Types

One benefit of the habitat type approach is that it integrates both MLD and nitrate availability in surface waters in defining phytoplankton habitats. Since DIN is often the limiting nutrient for phytoplankton in marine environments (Tyrell, 1999), understanding the sources and distribution of DIN in the study region provides a foundation for interpreting nitrogen dynamics in the entire planktonic food web. Based on the NAI values (Weber et al., 2019) derived from vertical profiles of nitrate concentration (Figure S5), nitrate availability was highest at MRW and some UpW stations, reaching measurable concentrations in surface waters. As expected, this indicates that both the Mekong River (Grosse et al., 2010) and coastal upwelling (Bombar et al., 2010) were important sources of nitrate for local plankton communities. Concurrently, MLD affected the supply of deep nitrate to surface waters, which can in turn greatly influence the composition of surface phytoplankton communities and may establish conditions favorable for N_2 fixation (Hutchins & Fu, 2017) when nitrogen is strongly limiting. For example, at OSW stations where MLD was deepest, the relative biomass of large diazotroph species was highest and could account for up to 20%–60% of total surface phytoplankton biomass (Figure 2a). We do note, however, that diazotrophs including unicellular groups (UCYN-A, -B, -C) were present and active in all habitat types (Hai Doan-Nhu, Rachel Foster, Sarah Weber, unpublished data). Taken together, a transition from MRW and UpW habitats to the OSW habitat reflects a shift from regions dominated by nitrate-utilization to one in which N_2 fixation was a common metabolic strategy and likely an important source of “new N.”

Using the $\delta^{15}\text{N}$ signatures of bulk POM and zooplankton biomass, we can track the input into the planktonic food web of major N sources that are isotopically unique—like riverine or upwelled nitrate ($\delta^{15}\text{N}$ of $\sim 5\text{‰}$) in contrast to diazotroph N ($\delta^{15}\text{N}$ of -2‰) (Montoya et al., 2002; Weber et al., 2017). The bulk $\delta^{15}\text{N}$ values of the five plankton compartments reflected the general trends described above, with the lowest $\delta^{15}\text{N}$ values at OSW stations where diazotrophs were common (Figure 2). The majority of these plankton bulk $\delta^{15}\text{N}$ values also correlated negatively and significantly with MLD (Figure 2), which gives strong evidence for the critical role of the MLD in governing the N sources utilized by the planktonic food web of the SCS.

Isotope mixing of nitrate and diazotroph nitrogen can account for the major trends in bulk $\delta^{15}\text{N}$ values of plankton, but transient processes like isotopic fractionation associated with the uptake of nitrate by phytoplankton must also be considered. Isotope theory (Montoya, 2007) predicts that when nitrate is injected into a system, for example by a river plume or upwelling, the isotopic composition of the nitrate pool will be modified through time as it is consumed and horizontally advected. Isotopic discrimination against ^{15}N during consumption ($\epsilon = 5\text{--}10\text{‰}$; Montoya & McCarthy, 1995; Waser et al., 1998) transfers N with a low $\delta^{15}\text{N}$ to phytoplankton biomass while simultaneously enriching the residual nitrate pool in ^{15}N . If much of this isotopically light phytoplankton nitrogen is subsequently removed from the system through sedimentation or grazing, assimilation of the residual, isotopically heavy nitrate will increase the $\delta^{15}\text{N}$ of the particulate pool. Both of these ^{15}N -depletion and ^{15}N -enrichment perturbations in the $\delta^{15}\text{N}$ of POM will lead to an apparent mismatch between the $\delta^{15}\text{N}$ of POM and zooplankton over the course of time of nitrate

consumption, as zooplankton act as a low-pass filter for changes in the isotopic composition of particles. If either perturbation signal in phytoplankton biomass persists long enough relative to the turnover times of zooplankton biomass, these nitrate fractionation signals will propagate up the food web into zooplankton. The extent of this signal propagation in turn provides a qualitative measure of the history of the fractionation process in the nitrate pool, which reflects the time course of environmental conditions experienced by the plankton community.

It is notable that these isotopic variations occurring in horizontal space through time in river plumes, for example, are analogous to those that occur vertically in the water column during an upwelling. In a steady-state system, the upward injection of subthermocline nitrate supports phytoplankton uptake that progressively increases the $\delta^{15}\text{N}$ of the residual nitrate toward the top of the nitracline (Altabet, 1996; Needoba et al., 2003) resulting in a strong gradient in the $\delta^{15}\text{N}$ of nitrate with depth. This nitrate fractionation mechanism must also take place in the water column off Viet Nam, producing an increase in nitrate $\delta^{15}\text{N}$ values of $>5.0\text{‰}$ above ~ 60 m at UpW stations (Figure S3). In consequence, phytoplankton can become enriched in ^{15}N due to the constant upward advection of subthermocline nitrate together with the constant isotope fractionation associated with its uptake.

Applying these concepts to our data set, we might expect to see both low and high plankton $\delta^{15}\text{N}$ measurements reflecting different stages of nitrate uptake at sites associated with major nitrate inputs. Indeed, we found very low $\delta^{15}\text{N}$ values in POM at sites of high nitrate availability in surface waters of the MRW and UpW type stations (Figure S6), but not in zooplankton (Figure 2). Since bulk $\delta^{15}\text{N}$ values below the subsurface nitrate value of 5.1‰ may be indicative of N from diazotrophy from fractionation in the early stages of nitrate consumption, or from recycling (Montoya et al., 1992, 2002), we cannot fully resolve the origin of these low $\delta^{15}\text{N}$ POM signatures. That being said, the contextual clues of high NAI and low $\delta^{15}\text{N}$ in POM without correspondingly low $\delta^{15}\text{N}$ in zooplankton point to a transient process related to nitrate uptake as the primary cause.

Conversely, when the plankton bulk $\delta^{15}\text{N}$ values are plotted against MLD, we did find one station where all the five plankton compartments (from integrated POM up through all four zooplankton compartments) were significantly enriched in ^{15}N , which was at OSW Stn. 6 situated on the fringes of the upwelling region (Figure S2). Evidence of sustained nitrate fractionation at an oligotrophic OSW habitat type station may seem counterintuitive, but the compilation of satellite SST images in Figure S2 indicates that the waters at Stn. 6 were likely advected from the upwelling region and had only recently shifted from the UpW to the OSW habitat type. In this situation, we would expect that shifts in the plankton community species and isotopic composition would lag behind changes in local chemical and physical properties so that the sampled plankton community retains the imprint of previous conditions. Weber et al. (2019) found evidence of such a delay in phytoplankton community in response to environmental change at a handful of stations, including Stn. 6. Taken together, the evidence at Stn. 6 points to a sustained input of isotopically enriched nitrate by upwelling into the local plankton food web followed by recent advection offshore.

Disregarding samples that were likely influenced by these nitrate fractionation processes (see Figure 2), we can now more reliably quantify the transfer of fixed nitrogen from diazotrophs into N pools of mesozooplankton using two-source stable isotope mixing approaches (Montoya et al., 2002). Diazotroph contributions to mesozooplankton biomass have only occasionally been quantified for some marine ecosystems like the tropical North Atlantic (Hauss et al., 2013; Landrum et al., 2011; Wannicke et al., 2010), the Amazon River plume (Loick-Wilde et al., 2016), the eastern Indian Ocean (Raes et al., 2014), the Baltic Sea (Loick-Wilde et al., 2019), and once previously in the southern South China Sea (Loick et al., 2007). So far, the highest measured transfer of diazotroph nitrogen into the upper planktonic food web was 67% in zooplankton from the tropical North Atlantic (Montoya et al., 2002). By comparison, the previously measured maximum of 13% for zooplankton in the SCS during SWM seasons was rather low (Loick et al., 2007), though the maximum value of 20% in this study indicates higher plasticity (Figure 3). The disparity in percentage diazotroph N input between bulk POM and zooplankton in this study (Figure 3) points to selective feeding in all habitats, such that diazotroph input to zooplankton is near 0% in coastal habitats despite evidence that diazotrophs were present and active. We also note that our approach may overestimate diazotroph N input into POM in areas where DIN was present and actively being drawn down (e.g., MRW stations and UpW Stn. 7), as discussed earlier. The minimal or low contribution of diazotroph N to mesozooplankton biomass

despite moderate to high inputs into POM may be related to the preferential grazing of the mesozooplankton as discussed below.

4.3. Zooplankton Diet and Environmental Regulation of the Planktonic Food Web Structure

As a complement to our bulk $\delta^{15}\text{N}$ measurements and to provide a more nuanced view of diet and trophic position within the plankton food web, we measured the compound-specific $\delta^{15}\text{N}$ signatures of AA in a subset of POM and mesozooplankton (1,000–2,000 μm) samples. By comparing AA $\delta^{15}\text{N}$ -Phe values across plankton compartments, we found much higher diazotroph N contributions to POM compared to mesozooplankton (Figure 4), which aligns well with results from our mixing model based on bulk $\delta^{15}\text{N}$ measurements (Figure 3). These results support previous findings from Loick et al. (2007), who used bulk $\delta^{13}\text{C}$ signatures to show that the POM collected on filters was largely unrepresentative of the mesozooplankton food source in this ecosystem. The lack of connectivity between these two pools may be due in part to the large diversity of phytoplankton cell sizes in the SCS. Zooplankton are known to selectively graze on phytoplankton according to cell size (Hansen et al., 1997), whereas the filtering process for sampling POM will sample all particles larger than the nominal filter pore size. As a result, the food source of a given size fraction of zooplankton likely represents only a portion of the bulk POM sampled. This in turn may explain why in regions such as the nutrient-limited subtropical North Atlantic, where detrital concentrations are probably lower and phytoplankton are likely smaller and more homogenous in size compared to phytoplankton in near coastal habitats (Rodríguez et al., 2001), filtered POM is much more representative of the mesozooplankton diet (Landrum et al., 2011).

On the scale of the habitat types, general trends in the $\delta^{15}\text{N}$ values of Phe_{zp} reflected those of bulk biomass for the 1,000–2,000 μm size fraction (Figure 5) and show a shift in N sources for biological production from nitrate toward an increase in diazotroph N inputs in oceanic waters where *Trichodesmium* spp. and other diazotrophs shaped the phytoplankton community (Figure 2a) (Weber et al., 2019). Interestingly, the change in N source across the habitats from nitrate-dependent toward higher diazotroph N input was associated with a lengthening of the food chain, given the inverse correlation of the N-source utilization measure $\delta^{15}\text{N}$ -Phe_{zp} with TP_{zp} (Figure 5). This phenomenon, which can also be viewed as a decrease in N-transfer efficiency through the food web, likely reflects a combination of two distinct factors: (a) the reduction in (non-diazotroph) phytoplankton cell sizes as conditions become more oligotrophic (Rodríguez et al., 2001), allowing for smaller consumers and more links in the food chain (Ryther, 1969); and (b) an enhancement in the routing of N through the microbial food web to consumers in communities where *Trichodesmium* spp. are more abundant (Mulholland, 2007). Most studies suggest that filamentous, N₂-fixing cyanobacteria like *Trichodesmium* spp. are not directly grazed by most zooplankton (Motwani et al., 2018; Mulholland, 2007; Wannicke et al., 2013) and that diazotroph N exuded or lysed from these communities in the form of ammonium or dissolved organic nitrogen (DON) enters zooplankton primarily through the microbial food web (Capone et al., 1997). According to trophic analyses of microbial food webs by Steffan et al. (2015), zooplankton should occupy carnivorous TPs when grazing on first level consumers from a microbial food web (but see also: Décima et al., 2017; Gutiérrez-Rodríguez et al., 2014). This indeed was the case during a highly degraded late stage of a filamentous cyanobacteria bloom in the Baltic Sea, when mesozooplankton clearly occupied carnivorous TPs (Loick-Wilde et al., 2018, 2019). However, most field studies from tropical oceans have found that mesozooplankton rarely reach the carnivorous threshold of TP ≥ 3 despite the presence of *Trichodesmium* spp., and instead tend to occupy a narrow range of TPs indicative of herbivore and omnivore dominance (Hannides et al., 2009; McClelland et al., 2003; Mompeán et al., 2016). This may be partly attributable to dietary flexibility in mesozooplankton outside of diazotroph bloom conditions. Additionally, net avoidance by larger, likely carnivorous zooplankton may also lower the TP in animals from $>1,000 \mu\text{m}$ size fractions (Clark et al., 2001; Kiørboe et al., 2014).

Our TP estimates from the SCS generally agree with the previously noted narrow ranges for tropical zooplankton, but TPs >2 were found at a handful of OSW stations (Stns. 5.16, 17, and 18) Table (1). At Stn. 18, detritivory played an important role in elevating TP_{zp}, but at these other two stations, an increasing reliance on carnivory supported indirectly by diazotrophy likely increased the mean TPs. At most OSW stations, however, mesozooplankton occupied an average TP closer to 2, reflecting a dominance of herbivory and a reduction in the role of the microbial pathway of diazotroph N delivery to zooplankton. The dominant

pathways of diazotroph N flow were likely direct grazing on diazotrophs other than *Trichodesmium* spp. (primarily DDAs and unicells; Conroy et al., 2016; Hunt et al., 2016; Loick-Wilde et al., 2016) and/or indirect inputs through grazing on non-diazotrophic autotrophs (Adam et al., 2016; Bonnet et al., 2016; Caffin et al., 2018; Klawonn et al., 2019) supported by diazotroph-derived DON and ammonium.

The multivariate analysis revealed a number of other interesting relationships among environmental variables and zooplankton bulk and amino acid-specific $\delta^{15}\text{N}$ measurements. The significant correlation between NAI and $\delta^{15}\text{N}\text{-Phe}_{\text{zp}}$ ($r^2 = 0.32$, $p < 0.05$, Figure 5) suggests that NAI, which has already been shown to be a robust indicator of nitrate availability to phytoplankton, is also a good indicator of N sources utilized by the higher plankton food web in the SCS and potentially in other systems. We also found that PO_4^{3-} correlated with $\delta^{15}\text{N}\text{-Phe}_{\text{zp}}$ ($r^2 = 0.67$, $p < 0.05$) and varied strongly and inversely with TP_{zp} ($r^2 = 0.41$, $p < 0.05$).

The statistical analyses additionally revealed that bulk and AA specific N isotope measures were not associated with temperature and salinity in the Mekong River plume and adjacent SCS. This result supports the findings of Weber et al. (2019), who showed that the majority of the system's environmental variability was explained by the integrative properties MLD, ChlMD, and NAI, and further supports the habitat type approach as a tool for analyzing plankton food web dynamics including higher trophic levels.

4.4. Ecosystem-Specific Trophic Enrichment in Mesozooplankton

The isotopic difference between trophic positions is called trophic enrichment (TE). It is a critical measure in biogeochemical models that reflects the mass and energy fluxes through food webs, but is difficult to quantify empirically (Post, 2002; Tiselius & Fransson, 2015). With the help of CSIA, the ecosystem-specific TE in mesozooplankton can now be estimated as the slope of the linear regression between zooplankton bulk $\delta^{15}\text{N}$ values corrected for the N source ($\Delta\delta^{15}\text{N}(\text{bulk-Phe})_{\text{zp}}$) and TP_{zp} (Mompéán et al., 2016). A slope of 3.0 in this regression would indicate a trophic enrichment of 3.0‰ in bulk biomass between TPs. This approach was applied to our data (Figure 6a) and to available CSIA data for mixed mesozooplankton from a variety of marine ecosystems (Figure 6b, Table S3). The significant linear regression between $\Delta\delta^{15}\text{N}(\text{bulk-Phe})_{\text{zp}}$ and TP_{zp} , implies a constant trophic enrichment of $\sim 5.1\text{‰}$ per trophic transfer in the SCS (Figure 6a). This value slightly exceeds the upper end of the 2.0–5.0‰ range typically measured for zooplankton (Post, 2002) and is considerably higher than the trophic enrichments of 2.7–3.7‰ measured for mesozooplankton from the Subtropical North Pacific, summertime Eastern Gotland Basin, summertime Baltic Proper, or Subtropical North Atlantic using the same method (Figure 6b, Table S3). Thus, our meta-analysis of TE estimates shows large variations in TE from field samples, ranging as low as 2.7‰ for mesozooplankton in the comparatively homogenous environment of the subtropical Pacific Ocean (Hannides et al., 2009) to 5.1‰ in the variable and dynamic waters off the coast of Viet Nam in the SCS and 6.3‰ in the transient upwelling off Oeland in the Baltic Sea (Loick-Wilde et al., 2019).

The mechanism(s) that modulates isotopic fractionation across trophic levels, and thus the surprisingly large range of TE values revealed through our meta-analysis, likely reflect the dietary quality of the available food as well as the basal metabolic costs associated with life in different habitats. The consensus from prior trophic enrichment studies is that TE is low when dietary N is near the requirements for optimal growth and high when dietary N either exceeds or is well below the optimum (Adams & Sterner, 2000; McCutchan et al., 2003; Vanderklift & Ponsard, 2003). Based on the findings from our analysis, we propose that TE magnitude is also related to ecosystem heterogeneity, such that plankton food webs in regions with high spatial and temporal variability in environmental conditions (e.g., river plumes and upwelling regions) are associated with a less efficient transfer of mass and energy across trophic levels. This hypothesis is consistent with the observation that zooplankton acclimate to the mean environment, which means a better fit between organism and environment in homogeneous areas and a poorer fit in heterogeneous areas where the mean condition might actually occur rarely or not at all. The time scale of variation is likely a critical factor in determining whether animals can optimize their feeding and acclimate their digestive processes to the available food (Hassett & Landry, 1990; Mayzaud et al., 1998) or their metabolic processes to environmental stressors like periodic shifts in salinity (Dutz & Christensen, 2018; Goolish & Burton, 1988; Van Someren Gréve et al., 2020).

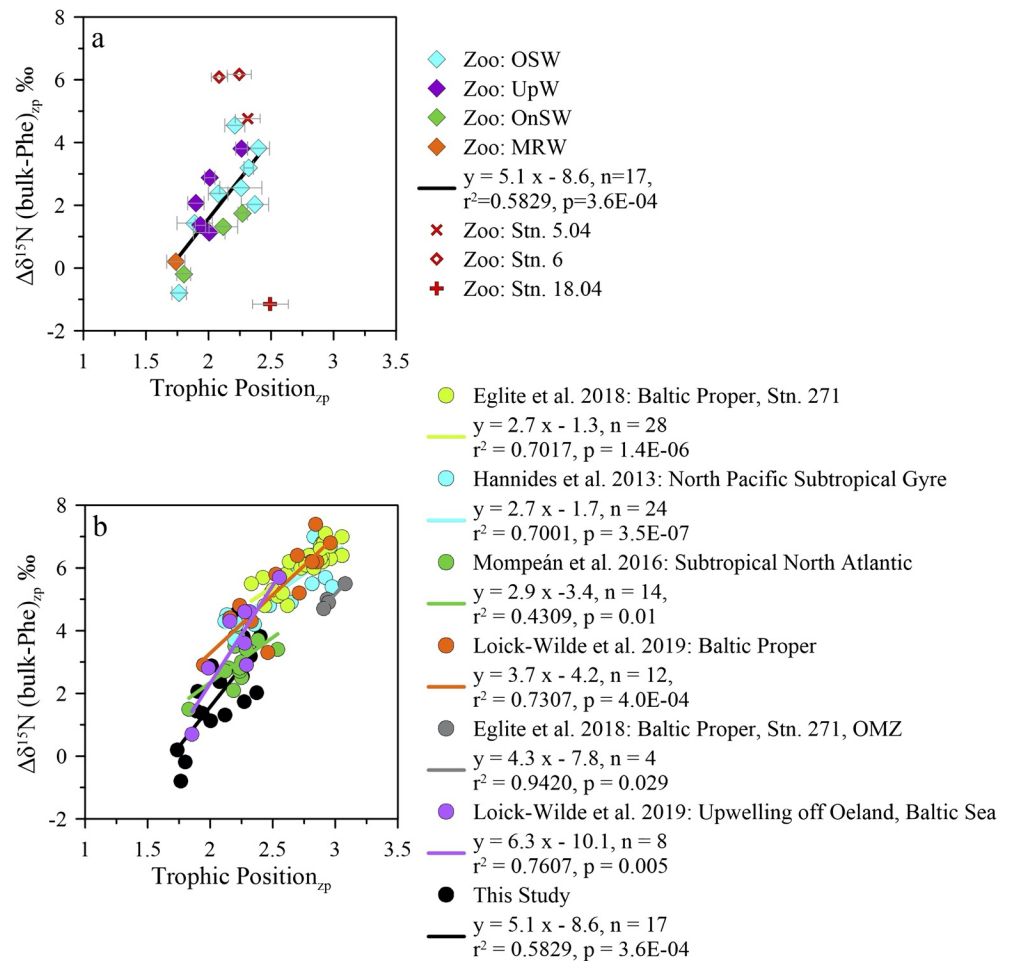


Figure 6. Calculation of ecosystem-specific trophic enrichment in mesozooplankton. (a) Comparison of $\Delta\delta^{15}\text{N}$ (bulk-Phe)_{zp} to TP_{zp} values for mesozooplankton (1,000–2,000 μm) from all South China Sea habitat types, where colors correspond to the habitat types as in Figure 1. Samples from Stns. 5.04, 6, and 18.04 were excluded as outliers from the regression analysis. (b) Comparison with metadata analysis of $\Delta\delta^{15}\text{N}$ (bulk-Phe)_{zp} versus TP_{zp} values from literature summarized in Table S3.

5. Conclusions

Our analysis provides convincing evidence that diazotrophy is prevalent in the offshore waters of the SCS, supporting up to 20% of zooplankton biomass during the early stages of the southwest summer monsoon season. Amino acid specific isotope analyses on mesozooplankton N uncovered a concurrent increase in mean TP with diazotroph-N dependence toward oligotrophic waters, a trend that was masked in the bulk $\delta^{15}\text{N}$ data by strong N-source isotope effects. These trends underscore recent findings that elevated mesozooplankton TPs are associated with diazotrophy, which may be in part due to the circuitous routing of diazotroph N through the food web. Mixed layer phosphate concentration also correlated strongly with mesozooplankton TP and may represent a useful indirect indicator of marine food web structure in near-coastal regions. Our analysis of mesozooplankton trophic enrichment estimates drawn from the available literature suggests a relationship between ecosystem heterogeneity and the less efficient transfer of mass and energy across trophic levels, providing new insights of this critical measure. Finally, with the help of the habitat type framework, we have shown that it is possible to tease apart critical plankton food web information in a highly variable environment, demonstrating the usefulness of this approach in studying physicochemically complex regions.

Data Availability Statement

Raw data of elemental and stable isotopes analyses are available at Dryad through <https://doi.org/10.5061/dryad.bk3j9kdbv> with a CC0 1.0 Universal (CC0 1.0) Public Domain Dedication license. Part of the data is available in Tables S1 and S2. This is a shared first-authorship between SCW and NL-W.

Acknowledgments

We thank the officers and crew of the R/V Falkor for their help and support at sea. This work was supported by the German Research Foundation (DFG Grant no. VO 487/11-1 to MV and LO 1820/4-1 to NL-W), the National Aeronautics and Space Administration (NASA Grant no. NNX16AJ08G to AS), the National Science Foundation (NSF Grant no. OCE-1737078 to JPM and OCE-1737128 to AS), as well as a shiptime grant by the Schmidt Ocean Institute. HD-N and LN-N would like to thank the National Foundation for Science and Technology Development (NAFOSTED) (Grant no. DFG106-NN.06–2016.78).

References

- Adam, B., Klawonn, I., Svedén, J. B., Bergkvist, J., Nahar, N., Walve, J., et al. (2016). N₂-fixation, ammonium release and N-transfer to the microbial and classical food web within a plankton community. *The ISME Journal*, *10*(2), 450–459. <https://doi.org/10.1038/ismej.2015.126>
- Adams, T. S., & Sterner, R. W. (2000). The effect of dietary nitrogen content on trophic level ¹⁵N enrichment. *Limnology & Oceanography*, *45*, 601–607. <https://doi.org/10.4319/lo.2000.45.3.0601>
- Altabet, M. A. (1996). Nitrogen and carbon isotopic tracers of the source and transformation of particles in the deep sea. In V. Ittekkot, P. Schäfer, S. Honjo, & P. J. Depetris (Eds.), *Particle flux in the ocean* (pp. 155–184). John Wiley & Sons.
- Bombar, D., Dippner, J. W., Doan, H. N., Ngoc, L. N., Liskow, I., Loick-Wilde, N., & Voss, M. (2010). Sources of new nitrogen in the Vietnamese upwelling region of the South China Sea. *Journal of Geophysical Research*, *115*(C6), C06018. <https://doi.org/10.1029/2008JC005154>
- Bonnet, S., Berthelot, H., Turk-Kubo, K., Fawcett, S., Rahav, E., L'Helguen, S., & Berman-Frank, I. (2016). Dynamics of N₂ fixation and fate of diazotroph-derived nitrogen in a low-nutrient, low-chlorophyll ecosystem: Results from the VAHINE mesocosm experiment (New Caledonia). *Biogeosciences*, *13*(9), 2653–2673. <https://doi.org/10.5194/bg-13-2653-2016>
- Butenschön, M., Clark, J., Aldridge, J. N., Allen, J. I., Artioli, Y., Blackford, J., et al. (2016). ERSEM 15.06: A generic model for marine biogeochemistry and the ecosystem dynamics of the lower trophic levels. *Geoscientific Model Development*, *9*(4), 1293–1339. <https://doi.org/10.5194/gmd-9-1293-2016>
- Caffin, M., Berthelot, H., Cornet-Barthaux, V., Barani, A., & Bonnet, S. (2018). Transfer of diazotroph-derived nitrogen to the planktonic food web across gradients of N₂ fixation activity and diversity in the western tropical South Pacific Ocean. *Biogeosciences*, *15*(12), 3795–3810. <https://doi.org/10.5194/bg-15-3795-2018>
- Capone, D. G., Zehr, J. P., Paerl, H. W., Bergman, B., & Carpenter, E. J. (1997). *Trichodesmium*, a globally significant marine cyanobacterium. *Science*, *276*(5316), 1221–1229. <https://doi.org/10.1126/science.276.5316.1221>
- Casciotti, K. L., Sigman, D. M., Galanter Hastings, M., Bohlke, J. K., & Hilkert, A. (2002). Measurement of the oxygen isotopic composition of nitrate in marine and fresh waters using the denitrifier method. *Analytical Chemistry*, *74*, 4905–4912. <https://doi.org/10.1021/ac020113w>
- Chao, S. Y., Shaw, P. T., & Wu, S. Y. (1996). El Niño modulation of the South China Sea circulation. *Progress in Oceanography*, *38*, 51–93. [https://doi.org/10.1016/S0079-6611\(96\)00010-9](https://doi.org/10.1016/S0079-6611(96)00010-9)
- Chikaraishi, Y., Ogawa, N. O., Kashiya, Y., Takano, Y., Suga, H., Tomitani, A., et al. (2009). Determination of aquatic food-web structure based on compound-specific nitrogen isotopic composition of amino acids. *Limnology and Oceanography: Methods*, *7*(11), 740–750. <https://doi.org/10.4319/lom.2009.7.740>
- Chikaraishi, Y., Ogawa, N. O., & Ohkouchi, N. (2010). Further evaluation of the trophic level estimation based on nitrogen isotopic composition of amino acids. In N. Ohkouchi, I. Tayasu, & K. Koba (Eds.), *Earth, life, and isotopes* (Vol. 415, pp. 37–51). Kyoto University Press.
- Clark, R. A., Frid, C. L. J., & Batten, S. (2001). A critical comparison of two long-term zooplankton time series from the central-west North Sea. *Journal of Plankton Research*, *23*(1), 27–39. <https://doi.org/10.1093/plankt/23.1.27>
- Conroy, B. J., Steinberg, D. K., Stukel, M. R., Goes, J. I., & Coles, V. J. (2016). Meso- and microzooplankton grazing in the Amazon River plume and western tropical North Atlantic. *Limnology & Oceanography*, *61*(3), 825–840. <https://doi.org/10.1002/lno.10261>
- Daewel, U., & Schrum, C. (2013). Simulating long-term dynamics of the coupled North Sea and Baltic Sea ecosystem with ECOSMO II: Model description and validation. *Journal of Marine Systems*, *119*, 30–49. <https://doi.org/10.1016/j.jmarsys.2013.03.008>
- Décima, M., Landry, M. R., Bradley, C. J., & Fogel, M. L. (2017). Alanine δ¹⁵N trophic fractionation in heterotrophic protists. *Limnology & Oceanography*, *62*(5), 2308–2322. <https://doi.org/10.1002/lno.10567>
- Dippner, J. W., Bombar, D., Loick-Wilde, N., Voss, M., & Subramaniam, A. (2013). Comment on “Current separation and upwelling over the southeast shelf of Vietnam in the South China Sea” by Chen et al. *Journal of Geophysical Research: Oceans*, *118*(3), 1618–1623. <https://doi.org/10.1002/jgrc.20118>
- Dippner, J. W., & Loick-Wilde, N. (2011). A redefinition of water masses in the Vietnamese upwelling area. *Journal of Marine Systems*, *84*(1–2), 42–47. <https://doi.org/10.1016/j.jmarsys.2010.08.004>
- Dippner, J. W., Nguyen, K. V., Hein, H., Ohde, T., & Loick, N. (2007). Monsoon induced upwelling off the Vietnamese coast. *Ocean Dynamics*, *57*, 46–62. <https://doi.org/10.1007/s10236-006-0091-0>
- Dutz, J., & Christensen, A. M. (2018). Broad plasticity in the salinity tolerance of a marine copepod species, *Acartia longiremis*, in the Baltic Sea. *Journal of Plankton Research*, *40*(3), 342–355. <https://doi.org/10.1093/plankt/fby013>
- Eglite, E., Graeve, M., Dutz, J., Wodarg, D., Liskow, I., Schulz-Bull, D., & Loick-Wilde, N. (2019). Metabolism and foraging strategies of mid-latitude mesozooplankton during cyanobacterial blooms as revealed by fatty acids, amino acids, and their stable carbon isotopes. *Ecology and Evolution*. Retrieved from <https://onlinelibrary.wiley.com/doi/abs/10.1002/ece3.5533>
- Eglite, E., Wodarg, D., Dutz, J., Wasmund, N., Nausch, G., Liskow, I., et al. (2018). Strategies of amino acid supply in mesozooplankton during cyanobacteria blooms: A stable nitrogen isotope approach. *Ecosphere*, *9*, e02135. <https://doi.org/10.1002/ecs2.2135>
- Ferrier-Pagès, C., Martinez, S., Grover, R., Cybulski, J., Shemesh, E., & Tchernov, D. J. M. (2021). Tracing the trophic plasticity of the coral–dinoflagellate symbiosis using amino acid compound-specific stable isotope analysis. *Microorganisms*, *9*(1), 182. <https://doi.org/10.3390/microorganisms9010182>
- Fry, B., & Quiñones, R. B. (1994). Biomass spectra and stable isotope indicators of trophic level in zooplankton of the northwest Atlantic. *Marine Ecology Progress Series*, *112*, 201–204. <https://doi.org/10.3354/meps112201>
- Fujii, T., Tanaka, Y., Maki, K., Saotome, N., Morimoto, N., Watanabe, A., & Miyajima, T. J. M. (2020). Organic carbon and nitrogen isoscapes of reef corals and algal symbionts. *Relative Influences of Environmental Gradients and Heterotrophy*, *8*(8), 1221. <https://doi.org/10.3390/microorganisms8081221>
- Gattuso, J.-P., Magnan, A., Billé, R., Cheung, W. W., Howes, E. L., Joos, F., et al. (2015). Contrasting futures for ocean and society from different anthropogenic CO₂ emissions scenarios. *Science*, *349*(6243), aac4722. <https://doi.org/10.1126/science.aac4722>

- Germain, L. R., Koch, P. L., Harvey, J., & McCarthy, M. D. (2013). Nitrogen isotope fractionation in amino acids from harbor seals: Implications for compound-specific trophic position calculations. *Marine Ecology Progress Series*, 482, 265–277. <https://doi.org/10.3354/meps10257>
- Gilbert, P. M., Middelburg, J. J., McClelland, J. W., & Jake Vander Zanden, M. (2019). Stable isotope tracers: Enriching our perspectives and questions on sources, fates, rates, and pathways of major elements in aquatic systems. *Limnology & Oceanography*, 64(3), 950–981. <https://doi.org/10.1002/lno.11087>
- Goering, J., Alexander, V., & Haubenstock, N. (1990). Seasonal variability of stable carbon and nitrogen isotopic ratios of organisms in a North Pacific bay. *Estuarine, Coastal and Shelf Science*, 30, 239–260. [https://doi.org/10.1016/0272-7714\(90\)90050-2](https://doi.org/10.1016/0272-7714(90)90050-2)
- Goolish, E. M., & Burton, R. S. (1988). Exposure to fluctuating salinity enhances free amino acid accumulation in *Tigriopus californicus* (Copepoda). *Journal of Comparative Physiology B*, 158(1), 99–105. <https://doi.org/10.1007/BF00692733>
- Grasshoff, K., Erhardt, M., & Kremling, K. (1983). *Methods of seawater analysis*. Verlag Chemie.
- Grosse, J., Bombar, D., Nhu Doan, H., Ngoc Nguyen, L., & Voss, M. (2010). The Mekong River plume fuels nitrogen fixation and determines phytoplankton species distribution in the South China Sea during low-and high-discharge season. *Limnology & Oceanography*, 55(4), 1668–1680. <https://doi.org/10.4319/lno.2010.55.4.1668>
- Gutiérrez-Rodríguez, A., Décima, M., Popp, B. N., & Landry, M. R. (2014). Isotopic invisibility of protozoan trophic steps in marine food webs. *Limnology & Oceanography*, 59(5), 1590–1598. <https://doi.org/10.4319/lno.2014.59.5.1590>
- Hannides, C. C., Popp, B. N., Choy, C. A., & Drazen, J. C. (2013). Midwater zooplankton and suspended particle dynamics in the North Pacific Subtropical Gyre: A stable isotope perspective. *Limnology & Oceanography*, 58(6), 1931–1946. <https://doi.org/10.4319/lno.2013.58.6.1931>
- Hannides, C. C., Popp, B. N., Landry, M. R., & Graham, B. S. (2009). Quantification of zooplankton trophic position in the North Pacific Subtropical Gyre using stable nitrogen isotopes. *Limnology & Oceanography*, 54(1), 50–61. <https://doi.org/10.4319/lno.2009.54.1.0050>
- Hansen, P. J., Bjornsen, P. K., & Hansen, B. W. (1997). Zooplankton grazing and growth: Scaling within the 2–2,000 μm body size range. *Limnology & Oceanography*, 42, 687–704. <https://doi.org/10.4319/lno.1997.42.4.0687>
- Hassett, R. P., & Landry, M. R. (1990). Seasonal changes in feeding rate, digestive enzyme activity, and assimilation efficiency of *Calanus pacificus*. *Marine Ecology Progress Series*, 62, 203–210. <https://doi.org/10.3354/meps062203>
- Hauss, H., Franz, J. M., Hansen, T., Struck, U., & Sommer, U. (2013). Relative inputs of upwelled and atmospheric nitrogen to the eastern tropical North Atlantic food web: Spatial distribution of $\delta^{15}\text{N}$ in mesozooplankton and relation to dissolved nutrient dynamics. *Deep Sea Research Part I: Oceanographic Research Papers*, 75, 135–145. <https://doi.org/10.1016/j.dsr.2013.01.010>
- Hofmann, D., Gehre, M., & Jung, K. (2003). Sample preparation techniques for the determination of natural $^{15}\text{N}/^{14}\text{N}$ variations in amino acids by gas chromatography-combustion-isotope ratio mass spectrometry (GC-C-IRMS). *Isotopes in Environmental and Health Studies*, 39, 233–244. <https://doi.org/10.1080/1025601031000147630>
- Hunt, B. P. V., Bonnet, S., Berthelot, H., Conroy, B. J., Foster, R. A., & Pagano, M. (2016). Contribution and pathways of diazotroph-derived nitrogen to zooplankton during the VAHINE mesocosm experiment in the oligotrophic New Caledonia lagoon. *Biogeosciences*, 13(10), 3131–3145. <https://doi.org/10.5194/bg-13-3131-2016>
- Hutchins, D. A., & Fu, F. (2017). Microorganisms and ocean global change. *Nature Microbiology*, 2(6), 17058. <https://doi.org/10.1038/nmicrobiol.2017.58>
- Jewett, L., & Romanou, A. (2017). Ocean acidification and other ocean changes. In D. J. Wuebbles, D. W. Fahey, K. A. Hibbard, D. J. Dokken, B. C. Stewart, & T. K. Maycock (Eds.), *Climate science special report: Fourth National climate assessment* (pp. 364–392). U.S. Global Change Research Program.
- Kiorboe, T., Jiang, H., Gonçalves, R. J., Nielsen, L. T., & Wadhwa, N. (2014). Flow disturbances generated by feeding and swimming zooplankton. *Proceedings of the National Academy of Sciences*, 111(32), 11738–11743. <https://doi.org/10.1073/pnas.1405260111>
- Klawonn, I., Bonaglia, S., Whitehouse, M. J., Littmann, S., Tienken, D., Kuypers, M. M. M., et al. (2019). Untangling hidden nutrient dynamics: Rapid ammonium cycling and single-cell ammonium assimilation in marine plankton communities. *The ISME Journal*, 13, 1960–1974. <https://doi.org/10.1038/ismej.2015.126>
- Landrum, J. P., Altabet, M. A., & Montoya, J. P. (2011). Basin-scale distributions of stable nitrogen isotopes in the subtropical North Atlantic Ocean: Contribution of diazotroph nitrogen to particulate organic matter and mesozooplankton. *Deep-Sea Research I*, 58, 615–625. <https://doi.org/10.1016/j.dsr.2011.01.012>
- Layman, C. A., Araujo, M. S., Boucek, R., Hammerschlag-Peyer, C. M., Harrison, E., Jud, Z. R., et al. (2012). Applying stable isotopes to examine food-web structure: An overview of analytical tools. *Biological Reviews*, 87(3), 545–562. <https://doi.org/10.1111/j.1469-185x.2011.00208.x>
- Loick, N., Dippner, J. W., Doan, H. N., Liskow, I., & Voss, M. (2007). Pelagic nitrogen dynamics in the Vietnamese upwelling area according to stable nitrogen and carbon isotope data. *Deep-Sea Research I*, 54, 596–607. <https://doi.org/10.1016/j.dsr.2006.12.009>
- Loick-Wilde, N., Fernández-Urruzola, I., Eglite, E., Liskow, I., Nausch, M., Schulz-Bull, D., et al. (2019). Stratification, nitrogen fixation, and cyanobacterial bloom stage regulate the planktonic food web structure. *Global Change Biology*, 25(3), 794–810. <https://doi.org/10.1111/gcb.14546>
- Loick-Wilde, N., Weber, S. C., Conroy, B. J., Capone, D. G., Coles, V. J., Medeiros, P. M., et al. (2016). Nitrogen sources and net growth efficiency of zooplankton in three Amazon River plume food webs. *Limnology & Oceanography*, 61(2), 460–481. <https://doi.org/10.1002/lno.10227>
- Loick-Wilde, N., Weber, S. C., Eglite, E., Liskow, I., Schulz-Bull, D., Wasmund, N., et al. (2018). De novo amino acid synthesis and turnover during N_2 fixation. *Limnology & Oceanography*, 63(3), 1076–1092. <https://doi.org/10.1002/lno.10755>
- Maar, M., Butenschön, M., Daewel, U., Eggert, A., Fan, W., Hjøllø, S. S., et al. (2018). Responses of summer phytoplankton biomass to changes in top-down forcing: Insights from comparative modelling. *Ecological Modelling*, 376, 54–67. <https://doi.org/10.1016/j.ecolmodel.2018.03.003>
- Martínez del Río, C., Wolf, N., Carleton, S. A., & Gannes, L. Z. (2009). Isotopic ecology ten years after a call for more laboratory experiments. *Biological Reviews*, 84(1), 91–111. <https://doi.org/10.1111/j.1469-185x.2008.00064.x>
- Mayzaud, P., Tirelli, V., Bernard, J. M., & Roche-Mayzaud, O. (1998). The influence of food quality on the nutritional acclimation of the copepod *Acartia clausi*. *Journal of Marine Systems*, 15, 483–493. [https://doi.org/10.1016/S0924-7963\(97\)00039-0](https://doi.org/10.1016/S0924-7963(97)00039-0)
- McCarthy, M. D., Benner, R., Lee, C., & Fogel, M. L. (2007). Amino acid nitrogen isotopic fractionation patterns as indicators of heterotrophy in plankton, particulate, and dissolved organic matter. *Geochimica et Cosmochimica Acta*, 71(19), 4727–4744. <https://doi.org/10.1016/j.gca.2007.06.061>
- McClelland, J. W., Holl, C. M., & Montoya, J. P. (2003). Nitrogen sources to zooplankton in the Tropical North Atlantic: Stable isotope ratios of amino acids identify strong coupling to N_2 -fixation. *Deep-Sea Research I*, 50, 849–861. [https://doi.org/10.1016/S0967-0637\(03\)00073-6](https://doi.org/10.1016/S0967-0637(03)00073-6)

- McClelland, J. W., & Montoya, J. P. (2002). Trophic relationships and the nitrogen isotopic composition of amino acids in plankton. *Ecology*, 83, 2173–2180. [https://doi.org/10.1890/0012-9658\(2002\)083\[2173:TRATNI\]2.0.CO;2](https://doi.org/10.1890/0012-9658(2002)083[2173:TRATNI]2.0.CO;2)
- McCutchan, J. H., Lewis, W. M., Jr., Kendall, C., & McGrath, C. C. (2003). Variation in trophic shift for stable isotope ratios of carbon, nitrogen, and sulfur. *Oikos*, 102(2), 378–390. <https://doi.org/10.1034/j.1600-0706.2003.12098.x>
- McMahon, K. W., McCarthy, M. D., Sherwood, O. A., Larsen, T., & Guilderson, T. P. (2015). Millennial-scale plankton regime shifts in the subtropical North Pacific Ocean. *Science*, 350(6267), 1530–1533. <https://doi.org/10.1126/science.aaa9942>
- Mompeán, C., Bode, A., Gier, E., & McCarthy, M. D. (2016). Bulk vs. amino acid stable N isotope estimations of metabolic status and contributions of nitrogen fixation to size-fractionated zooplankton biomass in the subtropical N Atlantic. *Deep Sea Research Part I: Oceanographic Research Papers*, 114, 137–148. <https://doi.org/10.1016/j.dsr.2016.05.005>
- Montoya, J. P. (2007). Natural abundance of ^{15}N in marine planktonic ecosystems. In R. Michener, & K. Lajtha (Eds.), *Stable isotopes in ecology and environmental science* (2nd ed., pp. 176–201). Blackwell.
- Montoya, J. P., Carpenter, E. J., & Capone, D. G. (2002). Nitrogen-fixation and nitrogen isotope abundances in zooplankton of the oligotrophic North Atlantic. *Limnology & Oceanography*, 47, 1617–1628. <https://doi.org/10.4319/lo.2002.47.6.1617>
- Montoya, J. P., & McCarthy, J. J. (1995). Nitrogen isotope fractionation during nitrate uptake by marine phytoplankton in continuous culture. *Journal of Plankton Research*, 17(3), 439–464. <https://doi.org/10.1093/plankt/17.3.439>
- Montoya, J. P., Wiebe, P. H., & McCarthy, J. J. (1992). Natural abundance of ^{15}N in particulate nitrogen and zooplankton in the Gulf Stream region and Warm-Core Ring 86A. *Deep-Sea Research*, 39(Suppl. 1), S363–S392. [https://doi.org/10.1016/S0198-0149\(11\)80020-8](https://doi.org/10.1016/S0198-0149(11)80020-8)
- Motwani, N. H., Duberg, J., Svedén, J. B., & Gorokhova, E. (2018). Grazing on cyanobacteria and transfer of diazotrophic nitrogen to zooplankton in the Baltic Sea. *Limnology & Oceanography*, 63(2), 672–686. <https://doi.org/10.1002/lno.10659>
- Mulholland, M. R. (2007). The fate of nitrogen fixed by diazotrophs in the ocean. *Biogeosciences*, 4(1), 37–51. <https://doi.org/10.5194/bg-4-37-2007>
- Needoba, J. A., Waser, N. A. D., Harrison, P. J., & Calvert, S. E. (2003). Nitrogen isotope fractionation by 12 species of marine phytoplankton during growth on nitrate. *Marine Ecology Progress Series*, 255, 81–91. <https://doi.org/10.3354/meps255081>
- Neumann, T., Fennel, W., & Kremp, C. (2002). Experimental simulations with an ecosystem model of the Baltic Sea: A nutrient load reduction experiment. *Global Biogeochemical Cycles*, 16(3), 1033. <https://doi.org/10.1029/2001gb001450>
- Ohkouchi, N., Chikaraishi, Y., Close, H. G., Fry, B., Larsen, T., Madigan, D. J., et al. (2017). Advances in the application of amino acid nitrogen isotopic analysis in ecological and biogeochemical studies. *Organic Geochemistry*, 113, 150–174. <https://doi.org/10.1016/j.orggeochem.2017.07.009>
- Paerl, H. W., & Huisman, J. (2008). Climate: Blooms like it hot. *Science*, 320, 57–58. <https://doi.org/10.1126/science.1155398>
- Peck, M. A., Arvanitidis, C., Butenschön, M., Canu, D. M., Chatzinikolaou, E., Cucco, A., et al. (2018). Projecting changes in the distribution and productivity of living marine resources: A critical review of the suite of modelling approaches used in the large European project VECTORS. *Estuarine, Coastal and Shelf Science*, 201, 40–55. <https://doi.org/10.1016/j.ecss.2016.05.019>
- Post, D. M. (2002). Using stable isotopes to estimate trophic position: Models, methods, and assumptions. *Ecology*, 83(3), 703–718. [https://doi.org/10.1890/0012-9658\(2002\)083\[0703:USITET\]2.0.CO;2](https://doi.org/10.1890/0012-9658(2002)083[0703:USITET]2.0.CO;2)
- Raes, E. J., Waite, A. M., McInnes, A. S., Olsen, H., Nguyen, H. M., Hardman-Mountford, N., & Thompson, P. A. (2014). Changes in latitude and dominant diazotrophic community alter N_2 fixation. *Marine Ecology Progress Series*, 516, 85–102. <https://doi.org/10.3354/meps11009>
- Rodriguez, J., Tintoré, J., Allen, J. T., Blanco, J. M., Gomis, D., Reul, A., et al. (2001). Mesoscale vertical motion and the size structure of phytoplankton in the ocean. *Nature*, 410(6826), 360–363. <https://doi.org/10.1038/35066560>
- Roy, T., Bopp, L., Gehlen, M., Schneider, B., Cadule, P., Frölicher, T. L., et al. (2011). Regional impacts of climate change and atmospheric CO_2 on future ocean carbon uptake: A multimodel linear feedback analysis. *Journal of Climate*, 24(9), 2300–2318. <https://doi.org/10.1175/2010JCLI3787.1>
- Ryther, J. H. (1969). Photosynthesis and fish production in the sea. *Science*, 166, 72–76. <https://doi.org/10.1126/science.166.3901.72>
- Schnitzer, A., & Steinberg, D. K. (2002). Active transport of particulate organic carbon and nitrogen by vertically migrating zooplankton in the Sargasso Sea. *Marine Ecology Progress Series*, 234, 71–84. <https://doi.org/10.3354/meps234071>
- Sigman, D. M., Casciotti, K. L., Andreani, M., Barford, C. M., Galanter, M., & Bohlke, J. K. (2001). A bacterial method for the nitrogen isotopic analysis of nitrate in seawater and freshwater. *Analytical Chemistry*, 73, 4145–4153. <https://doi.org/10.1021/ac010088e>
- Steffan, S. A., Chikaraishi, Y., Currie, C. R., Horn, H., Gaines-Day, H. R., Pauli, J. N., et al. (2015). Microbes are trophic analogs of animals. *Proceedings of the National Academy of Sciences*, 112(49), 15119–15124. <https://doi.org/10.1073/pnas.1508782112>
- Steffan, S. A., Chikaraishi, Y., Dharampal, P. S., Pauli, J. N., Guédot, C., & Ohkouchi, N. (2017). Unpacking brown food-webs: Animal trophic identity reflects rampant microbivory. *Ecology and Evolution*, 7(10), 3532–3541. <https://doi.org/10.1002/ece3.2951>
- Steinberg, D. K., & Landry, M. R. (2017). Zooplankton and the ocean carbon cycle. *Annual Review of Marine Science*, 9, 413–444. <https://doi.org/10.1146/annurev-marine-010814-015924>
- Steinberg, D. K., & Saba, G. K. (2008). Nitrogen consumption and metabolism in marine zooplankton. In D. G. Capone, D. A. Bronk, M. R. Mulholland, & E. J. Carpenter (Eds.), *Nitrogen in the marine environment* (pp. 1135–1196). Elsevier Academic Press. <https://doi.org/10.1016/b978-0-12-372522-6.00026-8>
- Thi Ha, D., Ouillon, S., & Van Vinh, G. (2018). Water and suspended sediment budgets in the lower Mekong from high-frequency measurements (2009–2016). *Water*, 10(7), 846. <https://doi.org/10.3390/w10070846>
- Tiselius, P., & Fransson, K. (2015). Daily changes in $\delta^{15}\text{N}$ and $\delta^{13}\text{C}$ stable isotopes in copepods: Equilibrium dynamics and variations of trophic level in the field. *Journal of Plankton Research*, 38(3), 751–761. <https://doi.org/10.1093/plankt/fbv048>
- Tyrell, T. (1999). The relative influences of nitrogen and phosphorus on oceanic primary production. *Nature*, 400, 525–531. <https://doi.org/10.1038/22941>
- Vanderklift, M. A., & Ponsard, S. (2003). Sources of variation in consumer-diet $\delta^{15}\text{N}$ enrichment: A meta-analysis. *Oekologia*, 136(2), 169–182. <https://doi.org/10.1007/s00442-003-1270-z>
- Van Someren Gréve, H., Jepsen, P. M., & Hansen, B. W. (2020). Does resource availability influence the vital rates of the tropical copepod *Apocyclops royi* (Lindberg, 1940) under changing salinities? *Journal of Plankton Research*, 42(4), 467–478. <https://doi.org/10.1093/plankt/fbaa031>
- Veuger, B., Middelburg, J. J., Boschker, H. T. S., & Houtekamer, M. (2005). Analysis of ^{15}N incorporation into D-alanine: A new method for tracing nitrogen uptake by bacteria. *Limnology and Oceanography: Methods*, 3(5), 230–240. <https://doi.org/10.4319/lom.2005.3.230>
- Voss, M., Bombar, D., Loick, N., & Dippner, J. W. (2006). Riverine influence on nitrogen fixation in the upwelling region off Vietnam, South China Sea. *Geophysical Research Letters*, 33, L07604. <https://doi.org/10.1029/2005GL025569>

- Wannicke, N., Korth, F., Liskow, I., & Voss, M. (2013). Incorporation of diazotrophic fixed N₂ by mesozooplankton—Case studies in the southern Baltic Sea. *Journal of Marine Systems*, 117–118, 1–13. <https://doi.org/10.1016/j.jmarsys.2013.03.005>
- Wannicke, N., Liskow, I., & Voss, M. (2010). Impact of diazotrophy on N stable isotope signatures of nitrate and particulate organic nitrogen: Case studies in the north-eastern tropical Atlantic Ocean. *Isotopes in Environmental and Health Studies*, 46(3), 337–354. <https://doi.org/10.1080/10256016.2010.505687>
- Waser, N. A. D., Harrison, P. J., Nielsen, B., Calvert, S. E., & Turpin, D. H. (1998). Nitrogen isotope fractionation during the uptake and assimilation of nitrate, nitrite, ammonium, and urea by a marine diatom. *Limnology & Oceanography*, 43(2), 215–224. <https://doi.org/10.4319/lo.1998.43.2.0215>
- Weber, S. C., Carpenter, E. J., Coles, V. J., Yager, P. L., Goes, J., & Montoya, J. P. (2017). Amazon River influence on nitrogen fixation and export production in the western tropical North Atlantic. *Limnology & Oceanography*, 62(2), 618–631. <https://doi.org/10.1002/lno.10448>
- Weber, S. C., Subramaniam, A., Montoya, J. P., Doan-Nhu, H., Nguyen-Ngoc, L., Dippner, J. W., & Voss, M. (2019). Habitat delineation in highly variable marine environments. *Frontiers in Marine Science*, 6, 112. <https://doi.org/10.3389/fmars.2019.00112>
- Wu, C.-R., Shaw, P.-T., & Chao, S.-Y. (1998). Seasonal and interannual variations in the velocity field of the South China Sea. *Journal of Oceanography*, 54(4), 361–372. <https://doi.org/10.1007/BF02742620>

References From the Supporting Information

- Chin, T. M., Vazquez-Cuervo, J., & Armstrong, E. M. (2017). A multi-scale high-resolution analysis of global sea surface temperature. *Remote Sensing of Environment*, 200, 154–169. <https://doi.org/10.1016/j.rse.2017.07.029>
- Doan-Nhu, H., Nguyen-Ngoc, L., Anh, N. T. M., Larsen, J., & Thoi, N. C. (2014). Diatom genus *Chaetoceros* Ehrenberg 1844 in Vietnamese waters. In J. P. Kociolek, M. S. Kulikovskiy, J. Witkowski, & D. M. Kharvud (Eds.), *Diatom research over time and space: Morphology, taxonomy, ecology and distribution of diatoms: From fossil to recent, marine to freshwater, established species and genera to new ones: Celebrating the work and impact of Nina Strelnikova on the occasion of her 80th birthday* (pp. 159–222). J. Cramer in der Gebr. Borntraeger Verlagsbuchhandlung.
- Fry, B. (2006). *Stable isotope ecology* (1st ed.). Springer.
- Guiry, M. D., & Guiry, G. M. (2020). *AlgaeBase*. World-Wide Electronic Publication. Retrieved from <http://www.algaebase.org>
- Menden-Deuer, S., & Lessard, E. J. (2000). Carbon to volume relationships for dinoflagellates, diatoms, and other protist plankton. *Limnology and Oceanography*, 45(3), 569–579. <https://doi.org/10.4319/lo.2000.45.3.0569>
- Montoya, J. P. (2008). Nitrogen stable isotopes in marine environments. In D. G. Capone, E. J. Carpenter, M. R. Mulholland, & D. A. Bronk (Eds.), *Nitrogen in the marine environment* (2nd ed., pp. 1277–1302). Academic Press. <https://doi.org/10.1016/b978-0-12-372522-6.00029-3>
- Round, F. E., Crawford, R. M., & Mann, D. G. (2007). *Diatoms: Biology and morphology of the genera*. Cambridge University Press.
- Sundström, B. G. (1986). *The marine diatom genus Rhizosolenia, a new approach to the taxonomy* (Doctor of Philosophy). Lund University. Retrieved from <http://www.marinespecies.org/aphia.php?p=sourcedetails&id=267626>
- Tomas, C. R. (1997). In C. R. Tomas (Ed.), *Identifying marine phytoplankton*. Elsevier Science.